SOME CONCEPTS IN REACTION DYNAMICS

Nobel lecture, December 8, 1986.

by
JOHN C. POLANYI
Department of Chemistry, University of Toronto, Toronto M5S 1Al. Canada

The objective in this work has been one which I have shared with the two other 1986 Nobel lectures, D. R. Herschbach and Y. T. Lee, as well as with a wide group of colleagues and co-workers who have been responsible for bringing this field to its current state. That state is summarized in the title; we now have some concepts relevant to the motions of atoms and molecules in simple reactions, and some examples of the application of these concepts. We are, however, richer in vocabulary than in literature. The great epics of reaction dynamics remain to be written. I shall confine myself to some simple stories.

1. EXPERIMENTAL AND THEORETICAL APPROACHES.

In this section I shall say something about the experimental and theoretical tools we have used, and give some indication of their origins.

Our principal experimental method has been the study of infrared chemiluminescence. The most valuable theoretical tool has been, and remains, the computer-integration of the classical equations of motion. Though both of these methods belong to the modern period of reaction dynamics, both have clear antecedents in earlier times.

Infrared chemiluminescence derives from the presence of vibrationally excited molecules in the products of reaction. Indirect evidence for the existence of such species was obtained by M. Polanyi and his co-workers in 1928 in the course of studies of the reactions of alkali metal atoms and halogens [1]. Following a suggestion by Bates and Nicolet [2], and by Herzberg [3], McKinley, Garvin, and Boudart [4] looked for and found visible emission from vibrationally excited hydroxyl radicals formed in the reaction of atomic hydrogen with ozone. This finding was followed soon after by the identification, by absorption spectroscopy, of vibrational excitation in the products of the reactions of atomic oxygen with NO_2 and ClO_2 [5].

Reference [5] appeared in the year that, in collaboration with J. K. Cashion, we undertook to look for infrared chemiluminescence from vibrationally excited hydrogen halides (and other hydrogen containing compounds) formed in simple exchange and addition reactions. The first reaction studied was that of atomic hydrogen with molecular halogens [6, 7]. Infrared emission was observed in the region 1.5-4.5 μm arising from the low-pressure ($\sim 10^{-3}$ torr) room temperature reaction,

$$H + X_2 \rightarrow HX\dagger + X \qquad (1)$$

where X was Cl or Br.

At that date there was lively discussion of the possibility of a visible analogue of the maser, that would operate on population-inverted electronic states (a working laser was still in the future) [8]. Given our interests it was natural to speculate about the properties of a vibrational laser. In our communication ("Proposal for an Infrared Laser Dependent on Vibrational Excitation") [9] we pointed to a number of virtues of such a device, of which we shall note two here.

(1) Provided that the vibrational temperature, T_V, sufficiently exceeds the rotational temperature, T_R, (both temperatures being positive, in contrast to the negative temperatures associated with population inversion in the discussions of that date) a large number of P-branch transitions will exhibit population inversion (fig. 1). We gave the name *`partial population inversion'* to this phenomenon, and noted that lasing based on partial population inversion could ensue shortly after a thermal pulse (arising from a pulsed arc, or shock wave), since 'partial cooling' would ensure $T_V >> T_R$. (2) A chemical reaction could be used to obtain either 'partial' or 'complete' population inversion. We were struck by the fact that the upper atmosphere could constitute a natural laser in the infrared favoured by its long path length and large number of partially population inverted transitions [9, 10].

Vibrational lasing was first achieved by Pate1 and co-workers [11]. Chemical reaction as the working material in a vibrational laser followed shortly afterward, through the work of Pimentel and his associates [12]. In both cases the major contribution to lasing came from partial population inversion, as indicated by the predominance of P-branch emission.

In our first communication regarding infrared chemiluminescence, we expressed the view that the method "promises to provide for the first time information concerning the distribution of vibrational and possibly rotational energy among the products of a three-centre reaction" [6]. This outcome was not so readily achieved.

By 1962 it was evident that reaction (1), despite the fact that it had proved to be a ready source of infrared chemiluminescence, converted its heat of reaction into vibration with the modest efficiency of ≤50% [13]. This finding met with scepticism, since it was pointed out, correctly, that it implied for the reverse endothermic process that one could have so much vibration in the reagents that the reaction probability would be markedly diminished [14]. The somewhat lame reply at that date was that "though odd, it could still be the case" [15].

Today we would surmise that it is the case since for the endothermic process $Cl + HCl \rightarrow Cl_2 + H$ a heavy particle (Cl) must approach during the brief time that the H-Cl bond remains extended; too much vibrational excitation can have the consequence that the Cl + HCl interaction is averaged over many vibrational periods, resulting in an 'adiabaticity' with respect to the flow of energy into the bond to be broken. At that date the importance of the relative timing of molecular motions (though recognised for other types of inelastic encounters) had not yet been documented for chemical reactions.

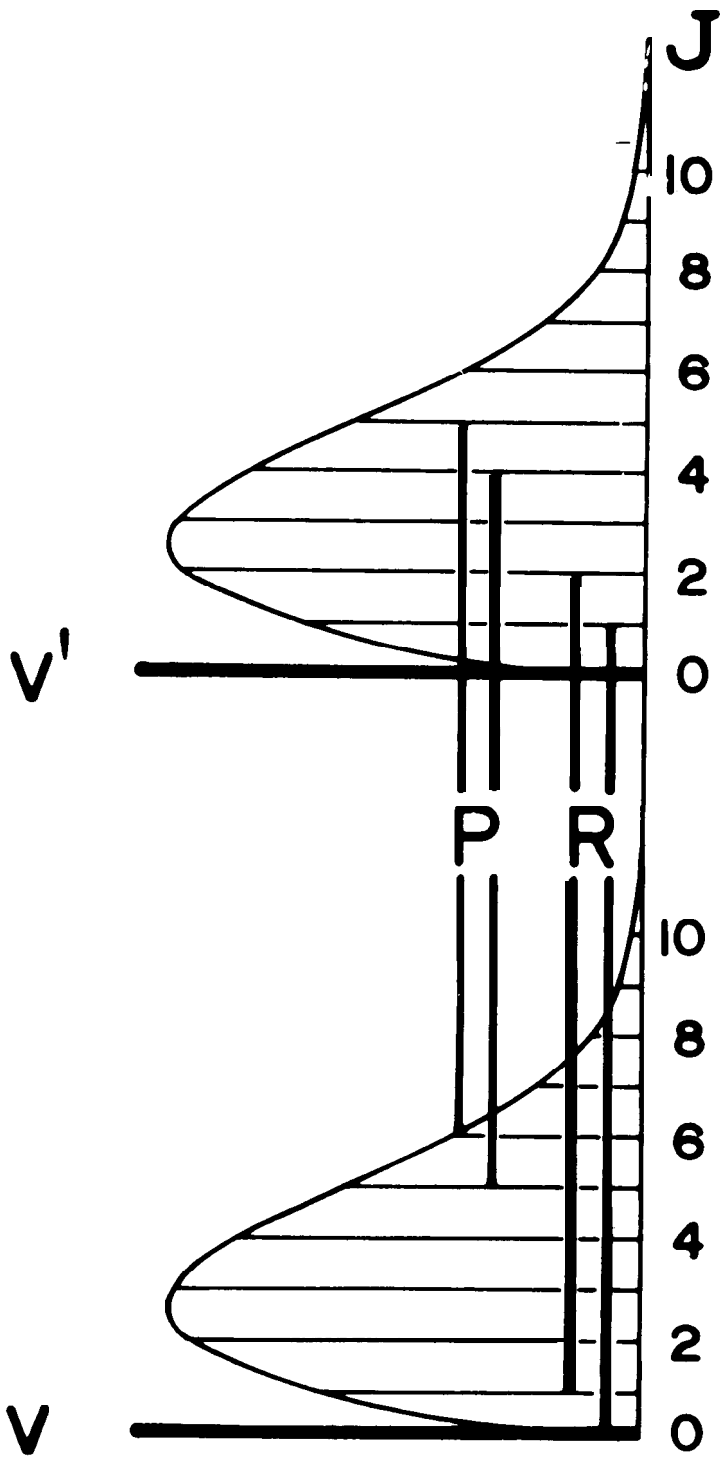

Figure 1. 'Partial population-inversion'; $T_V >> T_R (>O)$ ensures that the population in the upper state, N_u, exceeds that in the optically linked lower state, N_l for the indicated transitions (among others). The condition for lasing, $(N_u/g_u) > (N_l/g_l)$ where g is degeneracy, is only met for the P-branch. From J.C. Polanyi, Appl. Opt. Suppl. 2, 109 (1965); (also J. Chem. Phys. 34, 347 (1961)).

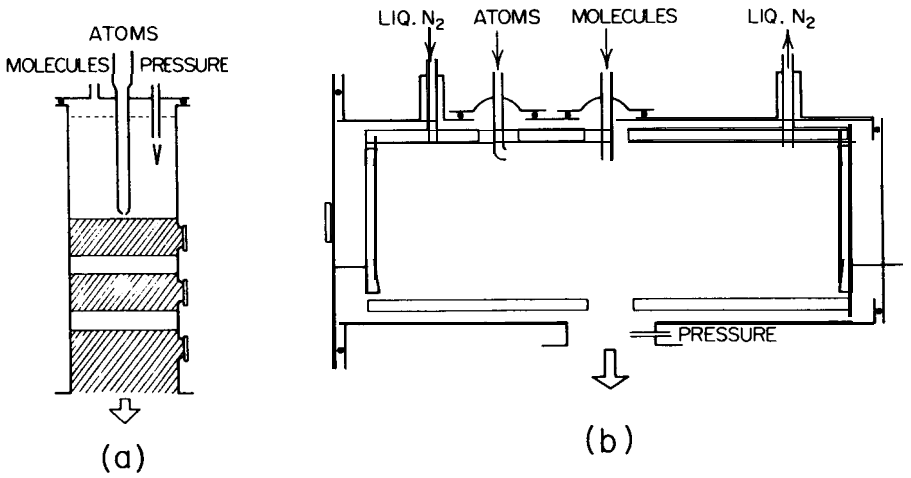

Figure 2. (a) Reaction vessel for 'Measured Relaxation' (MR) (shaded regions indicate internal reflective coating; three sapphire windows at successive sampling points are indicated at the right); (b) Reaction vessel for 'Arrested Relaxation' (AR) shown schematically (mirrors at either end of the vessel collect its radiation and bring it to the sapphire window at the left). From K.G. Anlauf et al., Disc. Faraday Soc. 44, 183 (1967).

It was not until 1967, with the development of the methods of "measured relaxation" (MR) [16] and "arrested relaxation" (AR) [16] that the goals established nine years earlier were truly achieved. The impediment to obtaining fully quantitative data by infrared chemiluminescence, or any other means, in regard to what we have termed the "detailed rate constants", k(V', R') (V' is the product vibrational excitation, and R' the product rotational excitation) has been the presence of an undetermined amount of vibrational and rotational relaxation of the reaction product prior to observation.

In the MR approach [16, 17-19], this was addressed by measuring the vibrational relaxation at points along the direction of flow, and hence correcting for this effect; see fig. 2 (a). In the AR method [16, 18-21], relaxation rather than being measured was arrested to the fullest extent possible, by the rapid removal of excited products. This was achieved by complete deactivation at a surface, usually cooled in the range 20-77K; fig. 1 (b). Arrest of relaxation yielded detailed rate constants at the level k(V',R',T'), where T' is the translational energy distribution in the newly-formed product, obtained by subtracting the initial vibrational plus rotational distributions from the total available energy.

Concurrently with the development of these infrared chemiluminescence techniques, the crossed molecular beam method was established as a quantitative tool, particularly by Herschbach and co-workers. This method obviated problems of relaxation by conducting reaction under single-collision conditions. Since the prime measurables were product angular and translational energy distributions, by 1967 a degree of overlap existed between the ap-

proaches. It was not, however, until the incorporation of universal detectors by Lee and Herschbach, following what we have come to know as the 'alkali age' of beam chemistry, that the same systems could be studied by both infrared chemiluminescence and molecular beam scattering.

By the time that the first quantitative data began to appear, powerful theoretical tools were available which could be used to link the potential field operating between atoms A, B, and C in a reaction

$$A + BC \rightarrow AB + C \qquad (2)$$

to the motions of the particles. In the original work on the London equation [22] by Eyring and Polanyi [23] an attempt was made, in collaboration with Wigner, to solve the classical equations of motion for the reactive system A + BC. This work was taken up by Hirschfelder and Wigner [24], but it was not until the first computer calculations of reaction dynamics by Wall, Hiller, and Mazur [25] that the full power of the approach became evident.

In parallel with Blais and Bunker [26] our laboratory [27] employed Wall's, Hiller's and Mazur's approach in an attempt to map out the major determinants of A + BC reaction dynamics. Both groups were inspired by the proposal made by M. G. Evans and M. Polanyi [28], over two decades earlier, that vibration in a newly-formed bond might originate from the release of reaction energy as the reagents approached. Detailed computation indicated that this suggestion embodied an important kernel of truth, though the full story, as might have been expected, revealed a substantially richer range of scenarios.

2. ENERGY DISTRIBUTION AMONG REACTION PRODUCTS

2.1 Experiment

In the MR method (see previous section), several observation windows for recording infrared (ir) chemiluminescence were located along the line of streaming flow. Provided that the observation windows were situated at distances corresponding to times during which relaxation was moderate, a simple graphical extrapolation back to zero time yielded adequate values for the relative k(v') (v' is the vibrational quantum number corresponding to the product vibrational energy V') [16, 17]. Detailed numerical analyses were also made, which included the effects of reaction, diffusion, flow, radiation, and collisional deactivation [17]. A model of this sort permitted, in effect, a more intelligent extrapolation to time t=0.

Subsequently the flow-tube approach was applied to the determination of vibrational energy distributions in a substantial number of infrared chemiluminescent reactions, particularly by Setser and his co-workers [29] and by Kaufman [30]. Infrared chemiluminescence experiments in flow tubes have also been extended to the elucidation of product energy-distributions from ion-molecule reactions [31].

In the A. R. method two uncollimated beams of reagent met in the centre of a vessel, exhibiting a background pressure, with reagents flowing, of $\sim 10^{-4}$-10^{-5} torr. Reaction occurred at the intersection of the beams (as demonstrated in ref. [18]). The products of reaction were transferred, following a few secondary

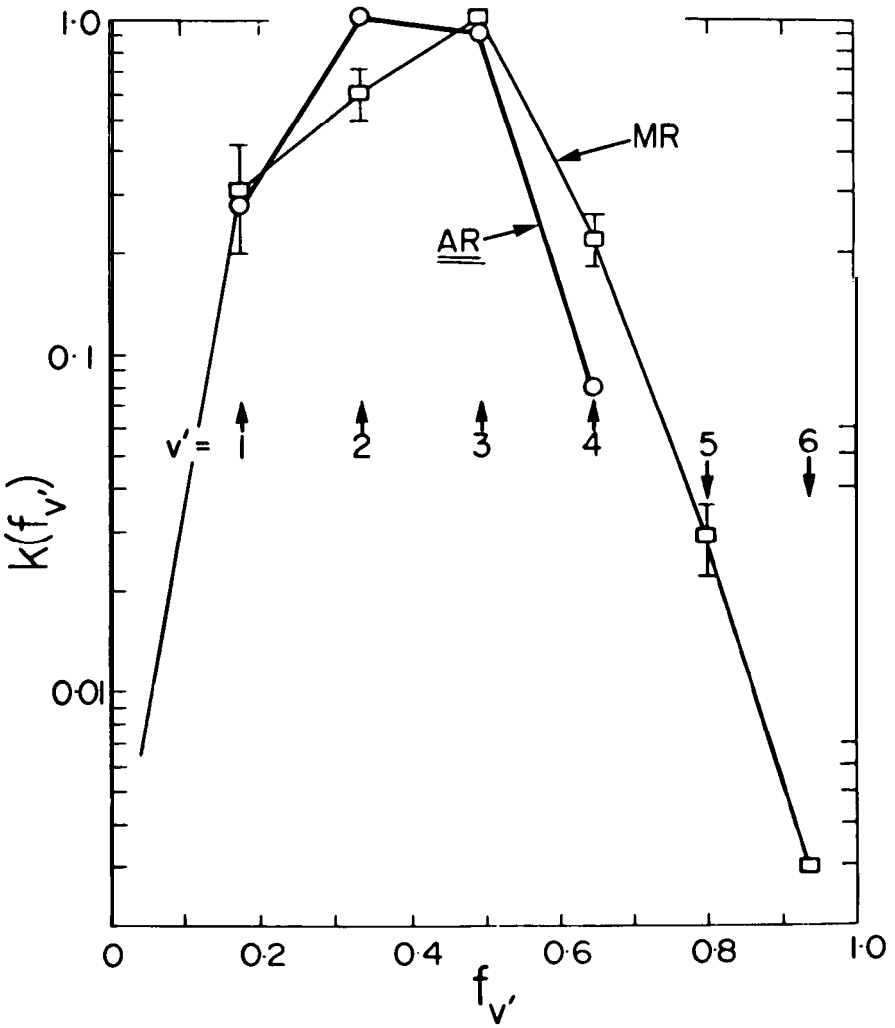

Figure 3. Semi-logarithmic plot of the probability that a fraction f_v, of the energy in the products of the reaction $H+Cl_2+$ HCI+Cl enters vibration in the newly-formed bond. The data were obtained independently by the MR and AR methods, as indicated. The vibrational quantum states v' = l-6 correspond to the values of f_v, indicated by arrows across the centre of the figure. From K.G. Anlauf et al., Disc. Faraday Soc. 44, 183 (1967).

collisions, to a deactivating surface which surrounded the reaction zone. Depending on the reagents, this surface acted as a cryo-pump, as a getter pump (trapping non-condensibles in excess condensible), or simply as an adsorber capable of bringing about complete vibrational deactivation (adsorbing product for a time sufficient to deactivate the material to its ground vibrational state, v=0).

The infrared chemiluminescence stemming from the small fraction of molecules that emitted early in their lifetimes, was collected by gold front-surface

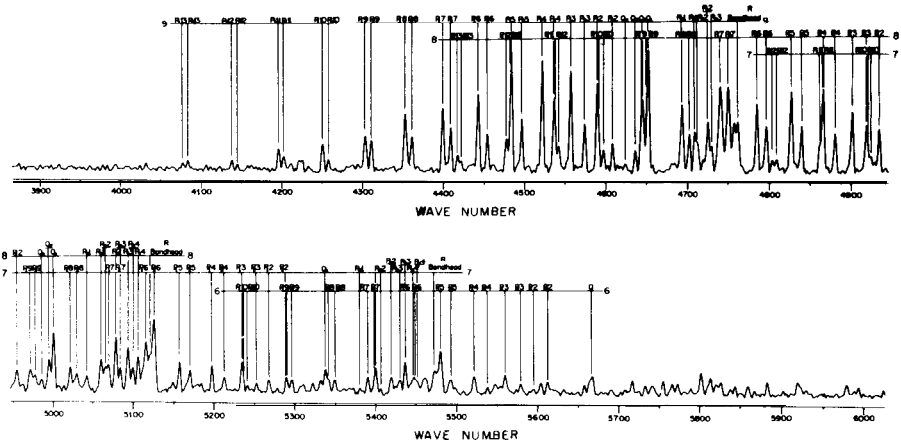

Figure 4. First-overtone ($\Delta v' = -1$) spectrum of OH formed in the reaction $H+0_3 \rightarrow OH+0_2$, $-\Delta H^\circ_o = 77$ kcal/mole. Under arrested relaxation conditions a continuous flow of reagents yields a steady-state distribution of OH(v') that increases with v' up to the highest accessible vibrational level, $v' = 9$ ($E(v' = 9) = 75$ kcal/mole, i.e. 3.25 eV). This spectrum was recorded by using a Fourier transform spectrometer and AR geometry; emission is from $v' = 6-9$ as indicated. From P.E. Charters et al., J. Appl. Optics, *10*, 1747 (1971); (also J.C. Polanyi and J.J. Sloan, Int. J. Chem. Kin. Symposium *1*, 51 (1975).

mirrors, freshly coated for each experiment; this procedure increased the effective solid angle being viewed by almost 50x [32]. By this means ~ 10^{-9} torr of vibrationally excited product could be detected in one v, J (vibrational) state, using the liquid-nitrogen cooled PbS semiconductor detectors that became available in the late 1950's. The emission spectrum (fig. 3) was recorded in early work on a (NaCl, then LiF) prism spectrometer, later on a grating spectrometer and (from the early 1970's, for e. g. [33]) on a variety of Fourier transform interferometric spectrometers.

The AR method was adopted by several laboratories, notably N. Jonathan's [34], D.W. Setser's [35], and J.D. McDonald's [36]. It is characterised by molecular flow of the reactants and hence low densities in the reaction zone, permitting observation of reaction products with highly non-Boltzmann rotational distribution, as well as non-Boltzmann vibrational distributions.

The effectiveness of the combination of molecular flow plus rapid removal of reaction products in reducing relaxation to an insignificant amount in the majority of systems studied was indicated by the fact that the steady-state distribution observed under these conditions was in satisfactory agreement with the initial vibrational distribution obtained by the MR method, (fig. 4) and the observed rotational distribution was largely unrelaxed, (fig. 5) indicating that collisional deactivation of vibrators-generally a less efficient process - was insignificant. In the case of a few very fast reactions (notably F + HBr $\rightarrow$ HF + Br [29]) k(v') from MR were at variance with those from AR. At the low flows used in the AR machine, it appears that reaction and deactivation were

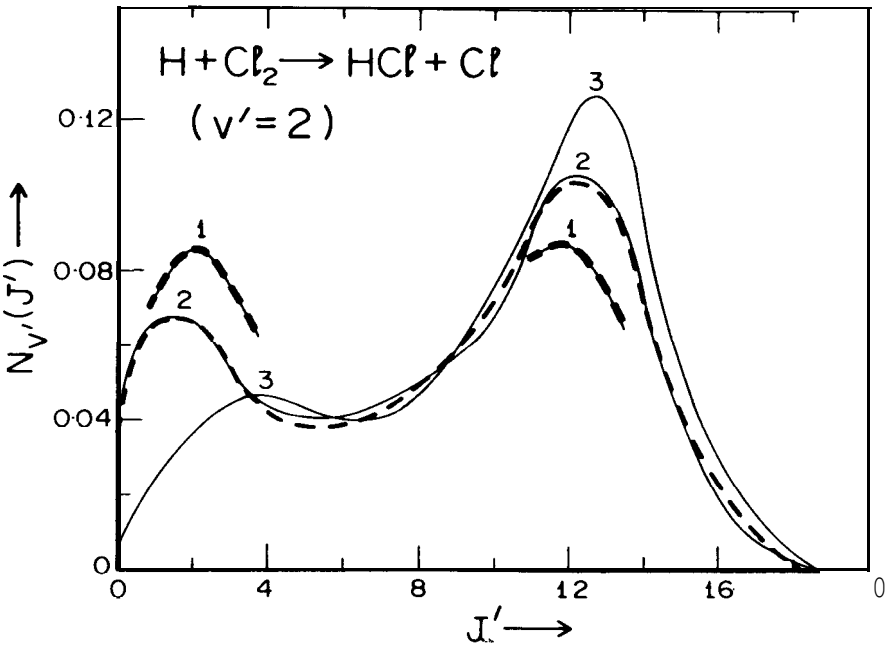

Figure 5. Solid lines record the decreasing contribution of the peak at low J′ to the observed rotational distribution (for $H+Cl_2$+HCl(v' = 2, J')+Cl) as the pressure in the beam-crossing region is decreased (in the sequence 3→2→1) in an A.R. vessel. The broken lines superimposed on the solid lines give relaxed distributions computed from 3. Based on fig. I of J.C. Polanyi and K:B. Woodall, J. Chem. Phys. *56,* 1563 (1972).

occurring within the inlets, invalidating the results [37]; in such a case the AR rotational distributions were also found to have been relaxed [38].

The observed rotational distributions were typically bimodal, comprising a non-thermal distribution at high rotational quantum number (high J') and a thermal distribution peaking at low J'. The contribution of the peak at low J' relative to that at high J' decreased with diminishing pressure in the reaction zone (fig. 5). Accordingly the low J' peak was ascribed to collisional relaxation, the relaxation mechanism being analyzed in detail [39].

Some detailed rate constants, k(v'), for the reaction

$$F + H_2 \rightarrow HF + H \qquad (3)$$

obtained by different procedures and by different workers are given in Table 1. Included among the methods used is one due to Pimentel and co-workers which made use of stimulated, rather than spontaneous, infrared emission [40]. This approach was an outgrowth of the first chemical laser, due to the same laboratory [12]. The laser approach [40] gave quantitative data concerning the population in the vibrational ground-state v′=0, which previously had been

Table I. Detailed rate constants, k(v') for $F+H_2 \rightarrow (HF(v')+H$; comparison data from various studies (with some variation in reagent collision energy).

	Reagt.Colln Energy	v'=1	v'=2	v'=3
Parker & Pimentel[1](1969)	539°K	0.18	1.00	–
Polanyi & Tardy[2](1969)	300°K	0.29	1.00	0.47
Jonathan et al.[3](1971)	300°K	0.28±0.02	1.00	058±0.12
Polanyi & Woodall[4](1972)	300°K	0.31	1.00	0.47
Coombe & Pimentel[5](1973)	236°K	–	1.00	0.505±0.01
	298°K	–	1.00	0.478±0.005
	364°K	–	1.00	0.463±0.006
	172°K	0.222±0.01	1.00	
	432°K	0.345±0.03	1.00	–
Chang & Setser[6](1973)	300°K	0.29	1.00	0.56
Berry[7](1973)	297°K	0.294±0.01	1.00	0.63±0.04
Perry & Polanyi[8](1976)	279°K	0.28	1.00	0.55
	718°K	0.38	1.00	0.55
	1315°K	0.44	1.00	0.55
Neumark et al.[9](1984)	1.84 kcal/mole	0.21	1.00	0.67

[1] J.H. Parker and G.C. Pimentel, J. Chem. Phys. *51,* 91 (1969).
[2] J.C. Polanyi and D.C. Tardy, ibid. *51,* 5717 (1969).
[3] N. Jonathan, C.M. Melliar-Smith, S. Okuda, D.H. Slater, and D. Timlin, Mol. Phys. *22,* 561 (1971).
[4] J.C. Polanyi and K.B. Woodall, J. Chem. Phys. *57,* 1574 (1972).
[5] R.D. Coombe and G.C. Pimentel, ibid. *59,* 251 (1973).
[6] H.W. Chang and D.W. Setser, ibid. *58,* 2298 (1973).
[7] M.J. Berry, ibid. *59,* 6229 (1979).
[8] D.S. Perry and J.C. Polanyi, Chem. Phys. *12,* 419 (1976).
[9] D.M. Neumark, A.M. Wodtke, G.N. Robinson, C.C. Hayden, and Y.T. Lee, J. Phys. *82,* 3045 (1985).

unobservable. Also included are the findings from crossed-molecular beam studies performed in Y.T. Lee's laboratory. In these demanding experiments the vibrational distribution was obtained from structure in the product translation energy-distribution, which was the measured quantity (the findings are for somewhat different reagent energy distributions than for the other experiments tabulated). The reaction $F + H_2 \rightarrow HF + H$ is of considerable fundamental interest since it involves only 11 electrons, and should therefore be amenable to *ab initio* computation (see below). The agreement between determinations of k(v') is satisfactory.

When these experiments and those described below were undertaken, quantitative data regarding k(v') did not exist. The prior observation of highly vibrationally excited reaction products noted in section 1, since it was a qualitative finding, left open the question of the form of k(v') which could have peaked anywhere from v'=0 to $v'=v'_{max}$ (the highest accessible vibrational state). In fact the distributions observed by ir chemiluminescence were found

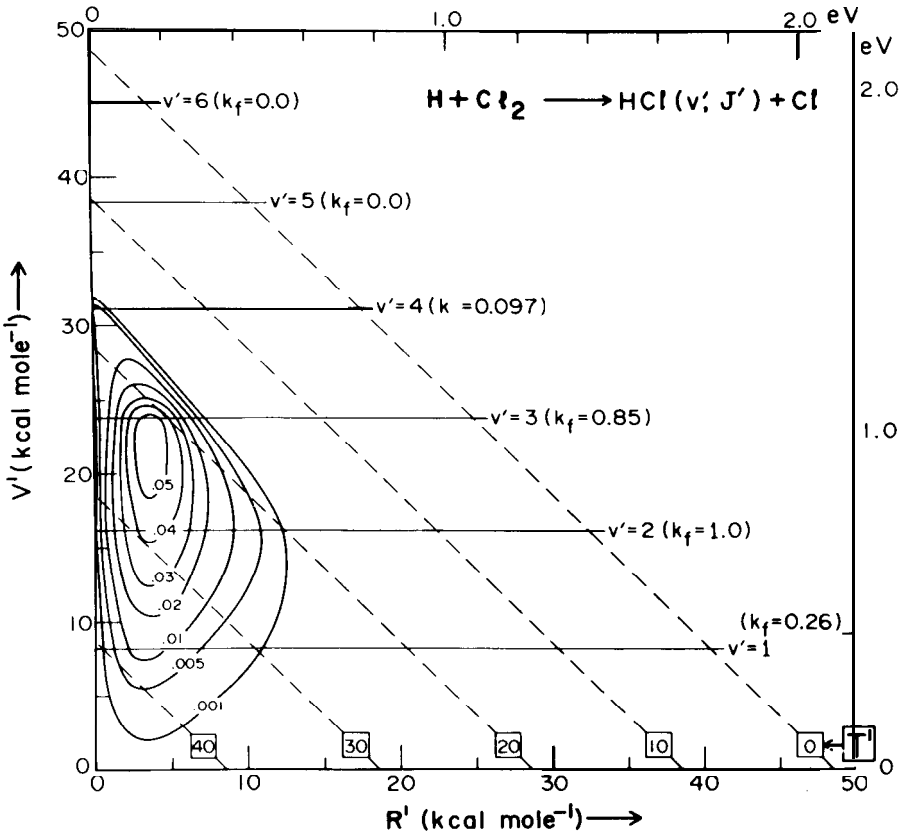

Figure 6. 'Triangle plot' for H+Cl_2HCl+Cl reaction showing the distribution of vibrational, rotational, and translational energy as contours of equal detailed rate constant k(V',R',T'). The ordinate is product vibrational energy, and the abscissa is the product rotational energy. Since the total available energy is approximately constant (E'_{tot} = 48.4 kcal/mole), translational energy, T', given by the broken diagonal lines, increases to 48.4 kcal/mole at V' = 0, R' = 0. The rate constant k_f = k(v') = Σ_j,k(v'J'); the subscript f denotes the 'forward', exothermic, direction. Contours have been normalized to k(v') = 1.00 where v'is the most-populated vibrational level. From K.G.Anlauf et al., J. Chem. Phys. 57, 1561 (1972).

to peak at intermediate v', so that the mean fraction of the available energy entering vibration in the new bond ranged from $< f'_v > = 0.39$ for H + Cl_2, $< f'_v > = 0.55$ for H + Br_2, $< f'_v > = 0.53$ for H + F_2, $< f'_v > = 0.66$ for F + H_2 up to $< f'_v > = 0.71$ for Cl + Hl and $< f'_v > \approx 0.9$ for H + $O_3 \rightarrow$ OH + 0_2.

An early finding was that the product vibrational energy distribution k(v') altered dramatically with isotopic substitution, but was roughly invariant if represented in the reduced form k(f'_v) [41]. This is what one would expect if classical mechanics applied rather than conservation laws involving quantum states. The finding gave us courage in applying classical mechanics to these reactions (despite the fact that they were characterised by widely spaced

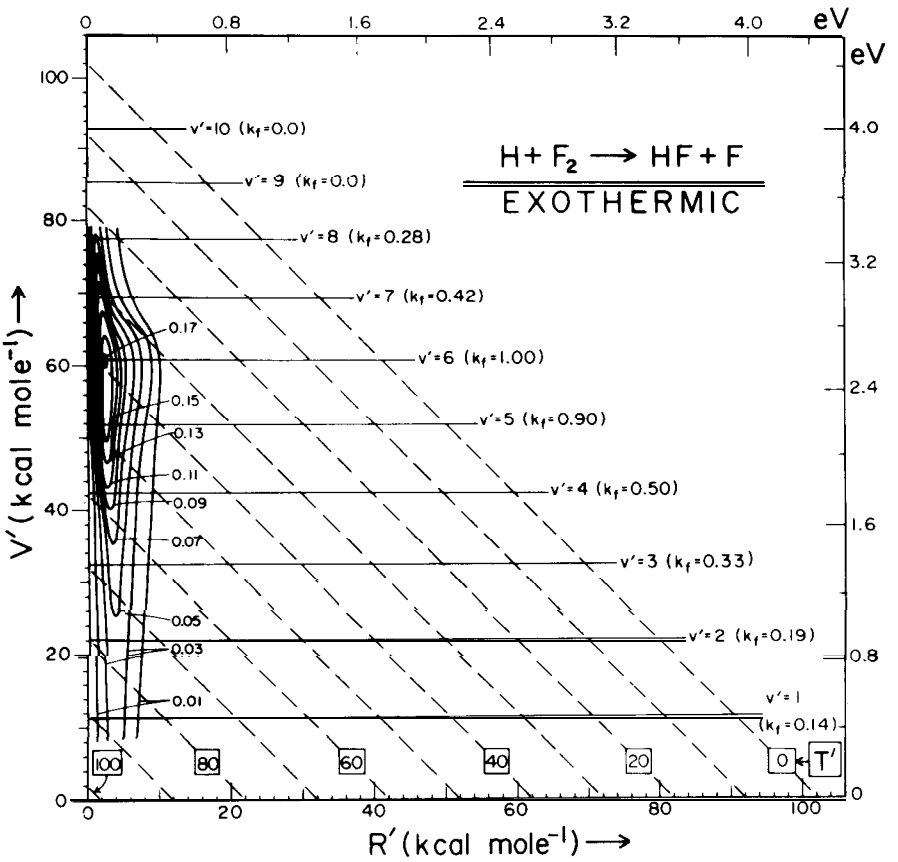

Figure 7. Triangle plot for $H+F_2 \rightarrow HF+F$ (see caption to fig. 6). E'_{tot} = 102 kcal/mole for this reaction. From J.C. Polanyi and J.J. Sloan, J. Chem. Phys. 57, 4988 (1972).

vibrational and rotational states), and also encouraged us to record our results in a graphical form that rode rough-shod over the quantised nature of k(v'J').

Four examples of the graphs that we have used (as a supplement to the tabulation of the actual k(v'J') values) as an aid to the visualisation of the experimentally determined product energy distributions, are shown in figs. 6-9. By interpolation between permitted combinations of V',R', and T', we obtain contours of equal k(V',R',T'). In these "triangle plots" contours are shown in V',R',T' space. They delineate a "hill" of detailed rate constant in that space. Portions of the hill that lie between vibrational energy states are merely included to guide the eye as to the breadth and shape of the product energy distribution over the axis' corresponding to V',R' and T'. Since classical mechanics is widely used in order to interpret energy distributions, these classical "fingerprints" of differing chemical reactions help us to picture contrasting types of behaviour.

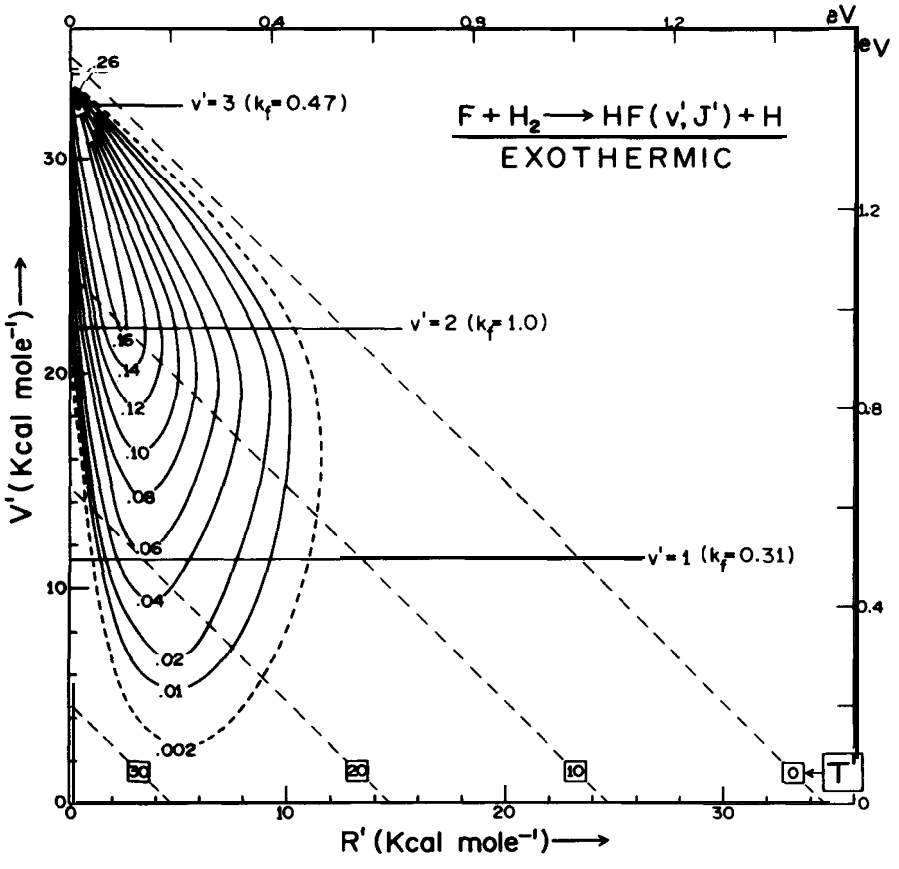

Figure 8. Triangle plot for $F+H_2 \rightarrow HF+H$ (see caption to fig. 6). E'_{tot} = 34.7 kcal/mole for this reaction. From J.C. Polanyi and K.B. Woodall, J. Chem. Phys. 57, 1574 (1972).

It is readily apparent that the first two reactions, H + Cl_2 and H + F_2 (figs. 6 and 7), though they liberate markedly different energies, both exhibit inefficient vibrational and rotational excitation and consequently efficient translational excitation. The third reaction, F + H_2 (fig. 8), gives rise to highly efficient vibrational excitation together with inefficient rotational excitation. The fourth reaction pictured, Cl + Hl (fig. 9), combines efficient vibrational excitation with exceptionally efficient rotational excitation ($< f_R' > = 0.13$ for Cl + Hl in contrast to $< f_R' > = 0.03$ for $H+F_2$). In concurrent work, alluded to in the following section, we linked these changes in dynamics to the release of repulsive energy in systems having differing mass combination and preferred geometries of the intermediate.

The ridge of the "detailed rate constant hill" is almost vertical in the case of the first reactions, moving out to higher R' at lower V' in the fourth of the reactions pictured (Cl + H_1), (for a tabulation of mean $< f_v' > <f_R' >$, $<f_T' >$, and the slope of the ridge $\Delta R'/\Delta V'$ for these reactions see table IV of

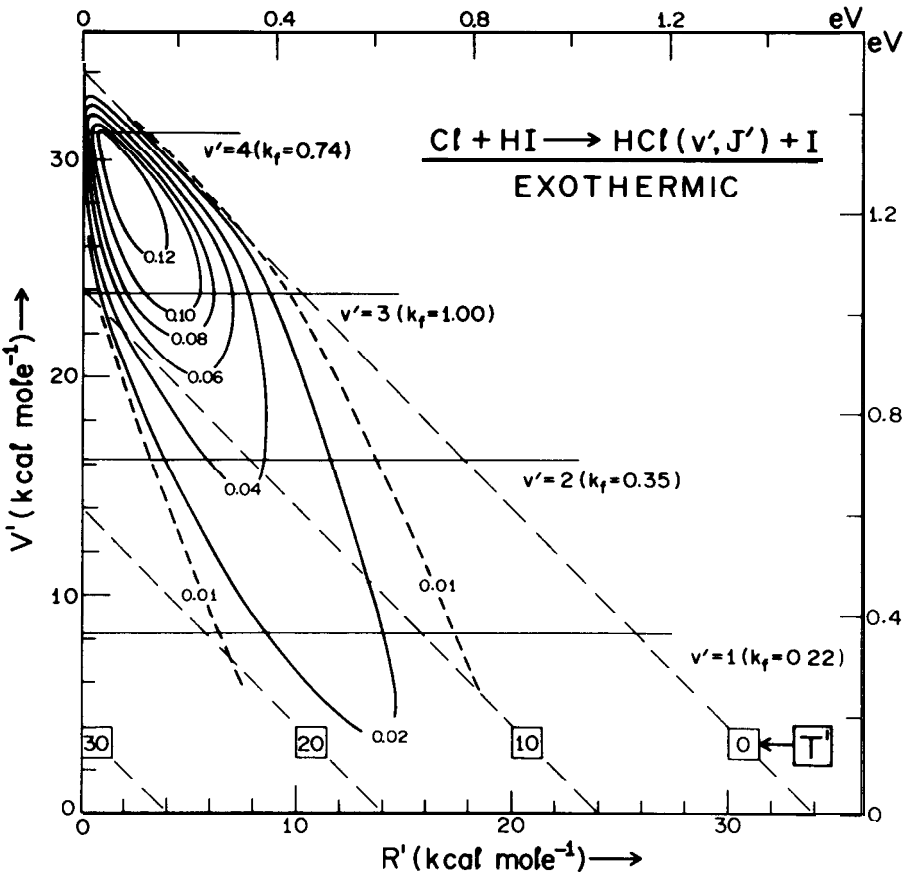

Figure 9. Triangle plot for Cl+HI+HCl+I. See caption to fig. 7. E'_{tot} = 34 kcal/mole. From D.H. Maylotte et al., J. Chem. Phys. 57, 1547 (1972).

ref. [21]) leaving aside the dynamical implications of this distinctive behaviour (see 2.2 below). It is noteworthy that successively lower vibrational states exhibit marked increases in *translational* energy in the first three cases, but a somewhat overlapped "translational energy spectrum" in the fourth case. This finding was seen to have interesting implications for the crossed molecular beam chemistry in which T' (as already noted) is the prime measurable. Figure 10 gives sample distributions over f_T' (blending rotational states into a continuum, since they cannot be resolved in molecular beam time-of-flight (tof) studies). The reaction H + F_2, not pictured here, gives rise to eight well-resolved translational peaks (fig. 5 of [21]). In the case of the F + H_2 reaction and its isotopic analogues in addition to resolving these peaks by tof, Y.T. Lee's laboratory have in recent times fully characterised the angular distribution of each [42].

The triangle plots, exemplified in figs. 6-9, constitute one way of "compacting" the substantial data embodied in k(v'J',T'). The information-theory,

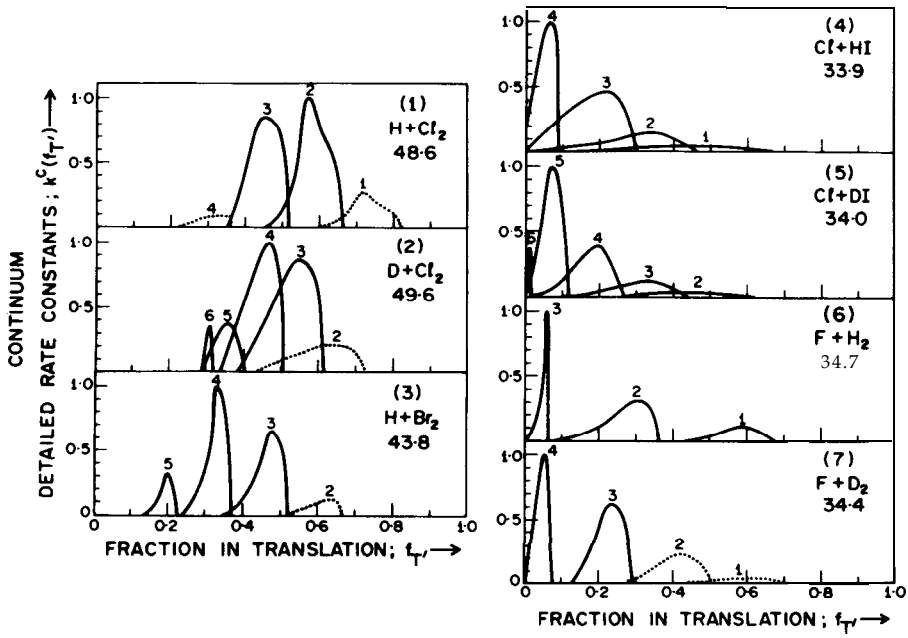

Figure 10. Translational energy-distribution in the products of some exchange reactions A+BC→AB+C obtained by subtracting the vibrational excitation measured by its chemiluminescence from the total product energies (indicated in the figure). The vibrational states that contribute to the translational peaks are recorded above each peak. From K.G. Anlauf et al. J. Chem. Phys. *53,* 4091 (1970).

pioneered by Bernstein and Levine [43], has provided a widely-used alternative method of compaction in terms of parameters which describe the deviation of the observed vibrational and rotational distributions from a statistical outcome. These deviations can be described as vibrational and rotational "surprisals". In those cases for which the surprisal is found to be a linear function off, or f'_R, not only can the data be reduced to only two constants, but extrapolations can be made. We have made use of this in our work in order to estimate the (small)-fraction of product formed in the non-emitting state, v'=0.

Figure 11 contrasts the triangle plots for HF (fig. 11 (a)) and DF (fig. 11 (b)) formed in the thermal reaction F+HD → HF(v'J') or DF(v'J') (+D or +H) [44]. These data are included since they shed light on a source of product rotational excitation. The forces operating are very similar but are clearly substantially more effective in rotationally exciting HF (mean fraction of the available energy entering rotation is $\langle f'_R \rangle = 0.125$) than DF($\langle f'_R \rangle = 0.066$). We postpone discussion to section 2.2 below.

It is interesting to note that for the family of reactions F+HD → HF, F+HD → DF, F+H_2, F+D_2 studied by ir chemiluminescence, the first reaction in the list exhibited vibrational excitation that was anomalously low as compared with classical calculation. This (together with the reagent-energy dependence

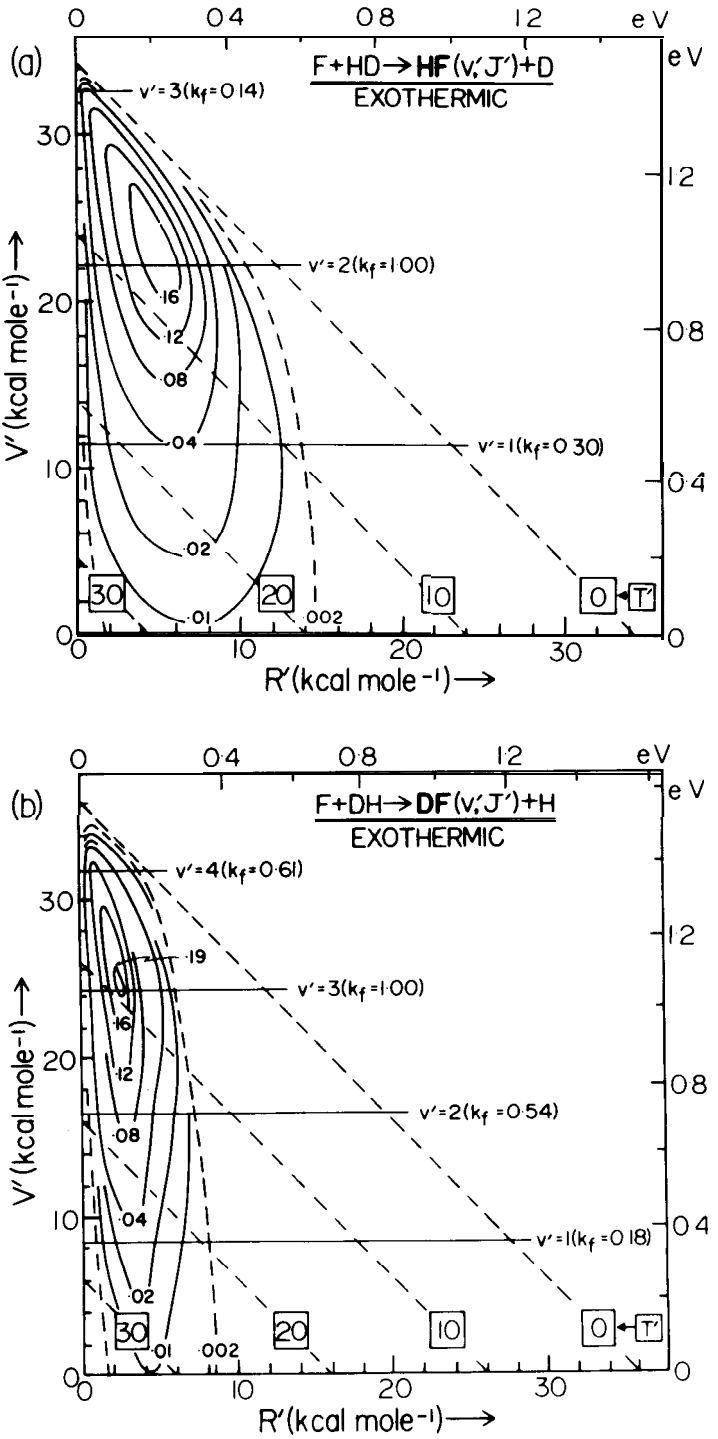

Figure 11. Triangle plots for both branches of the F+HD exchange reaction. The total available energy in the products was taken to be E'_{tot} = 34.3 kcal/mole for the HF product, and E'_{tot} = 36.1 kcal/mole for DF, in calculating product translation T′. From D.S. Perry and J.C. Polanyi, Chem. Phys. 12. 419 (1976).

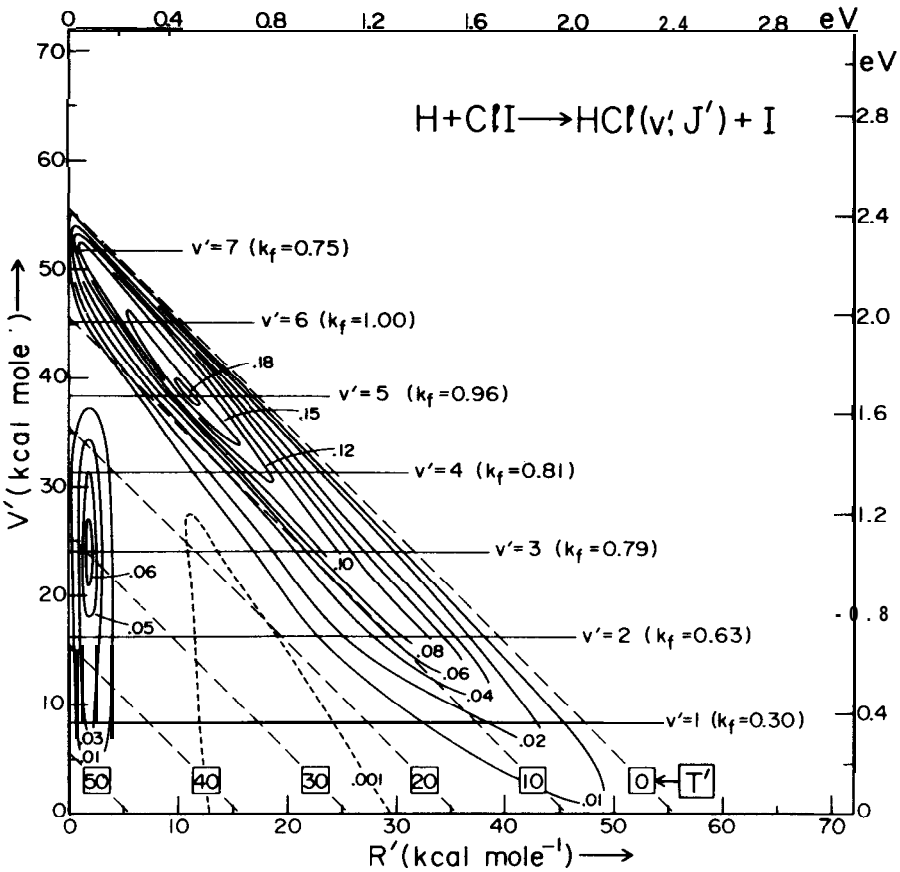

Figure 12. Triangle plot for the reaction H+ClI at 300K showing bimodality (18 % of the HCl is in the low -J' mode, 82% in the high -J'). From M.A. Nazar, J.C. Polanyi, and W.J. Skrlac, Chem. Phys. Letts. 29, 473 (1974). See also J.C. Polanyi and W.J. Skrlac, Chem. Phys. 23, 167 (1977).

of k(v'=3)) was taken to be evidence of a quantum effect at the threshold energy for formation of HF(v'=3). Molecular beam experiments in Y.T. Lee's laboratory have shown the importance of quantum effects on the dynamics of the first member of this family of reactions [42].

Figure 12 shows the dramatic influence the atom C can have on the dynamics of a reaction A+BC → AB+C. Superficially the reaction illustrated resembles H+ClY→ HCl+Y, for which the detailed rate constant k(V',R',T') is given in fig. 6; the difference is that the second halogen atom, Y, has been changed from Y=Cl to Y=I, with the effect on k(V',R',T'), recorded in fig. 12. Bimodal product energy distributions were also observed in a number of other studies [45-48] and were regarded as indicative of the existence of two types of reaction dynamics leading to the identical product (HCl in the case illustrated). This phenomenon was termed 'microscopic' branching, to distinguish it from the 'macroscopic' branching leading to chemically different products (see

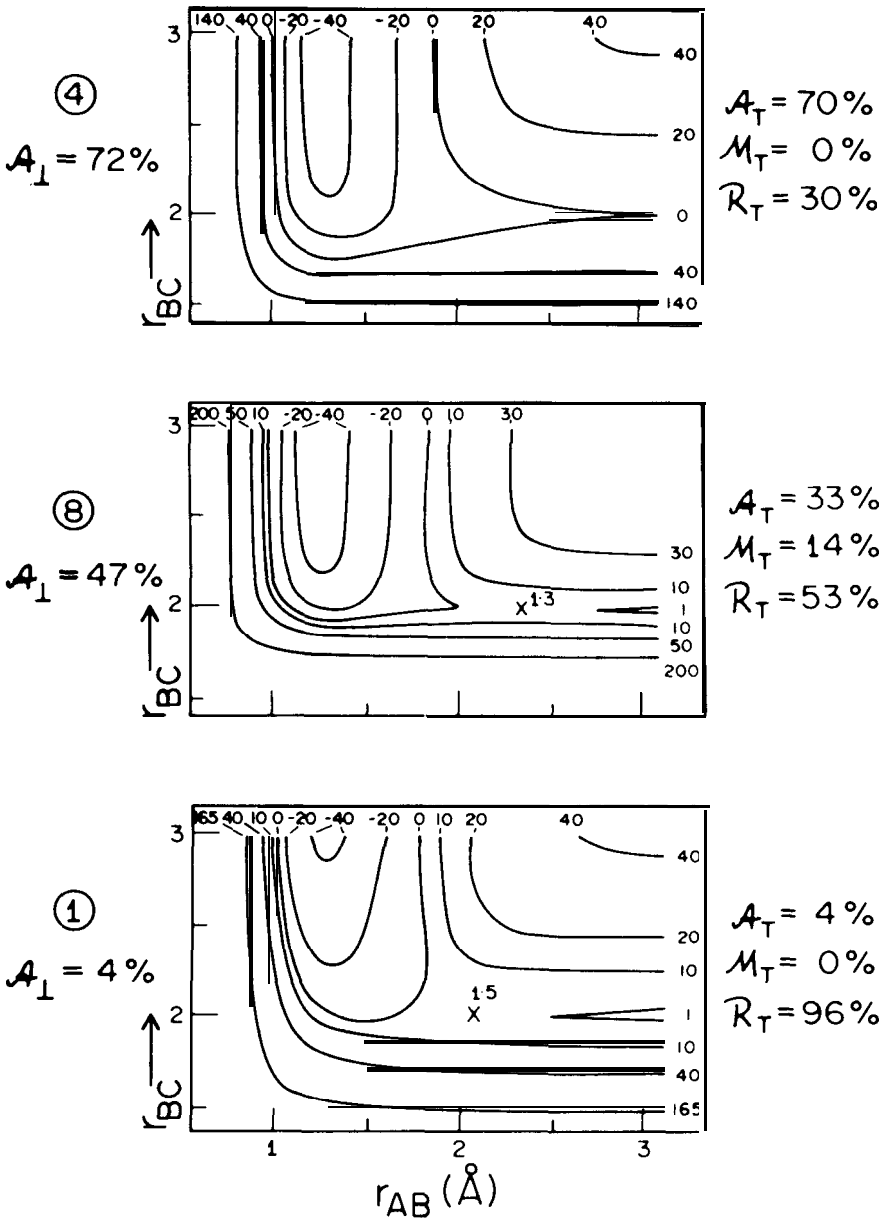

Figure 13. Three potential-energy surfaces (pes) illustrative of the changes in potential energy as reagents A+BC (lower right) pass through collinear transition states A-B-C to form products AB+C (upper left). Contour energies are in kcal/mole; all three reactions have the same exothermicity. The pes, designated 1, 8, and 4, are arranged vertically in order of increasing "attractiveness". The pes are indexed at the left according to the percentage attractive energy-release taken from a perpendicular path across the surface (A ⊥ = 4, 47, and 72 % for surfaces 1, 8, and 4). The same pes are described at the right according to the percentage attractive, mixed and repulsive energy release, A_T,M_T, and R_T, along a single collinear trajectory; this designation depends upon mass combination, which was L+HH (L = 1 amu, H = 80 amu). The barrier crest. designated x, shifts to "earlier" locations along r_{AB} as the surfaces become more attractive. Excerpted from P.J. Kuntz et al., J. Chem. Phys. 44, 1168 (1966).

for example fig. 11). As we shall indicate in section 2.2, these two types of branching are linked.

It is interesting to consider the strengths and weaknesses of ir spectroscopy as a tool in the study of reaction dynamics. The major limitations have stemmed from the low transition probabilities in the ir, the insensitivity of ir detectors, and the lack of a sufficiently precise timescale against which to measure the vibrational and especially rotational relaxation. Substantial improvements in sensitivity have been achieved using the important new methods of laser-induced fluorescence (LIF) [48] and resonantly enhanced multiphoton ionization (REMPI) [49]. However, since these make use of electronic transitions, they cannot so readily scan the full manifold of product vibrotational energy states to yield data as complete as that exemplified in figs. 7-9, which remains the most complete available.

Tunable ir lasers, combined with adequate time-resolution, could give a new lease of life to the vibrotational spectroscopy of reaction products. A promising development employing ir chemiluminescence is the introduction of time-resolved fourier transform spectroscopy following the pulsed photolytic initiation of exchange reaction [50].

2.2 Theory

The origin of these theoretical studies is outlined in section 1, above. In the early 1960's two groups [26, 27] became interested in using the computer-based classical trajectory method [25] (often called the Monte Carlo approach) to explore, for the first time, a suggestion made over two decades earlier [28], that energy released as reagents approach is responsible for vibration in the newly-formed bond.

Figure 13 shows three potential-energy surfaces (pes), all of a modified London, Eyring, Polanyi, Sato (LEPS) variety [27, 52, 53], selected from a wider group examined in ref. [53]. The energy released as the reagents approached (termed the attractive energy release, and defined as $A_{\perp}$ or A_{τ} [53, 54]; see the caption of fig. 13) increases as one moves upwards in the figure. There is, in related families of reaction, a concurrent diminution in the height of the energy-barrier, and a shift of the barrier to earlier locations along the coordinate of approach with increased A. It has proved possible to give an empirical expression to these correlations [55, 56].

In fig. 14 it can be seen that for a group of 8 pes moderate percentages of energy release along the coordinate of approach (% A $\perp$) are converted quantitatively into product vibration for a particular reagent mass combination (L+HH; see caption). For high % $A\perp$ the reaction moves into a new regime in which product vibration decreases with increased attractive energy release. Examination of the trajectories indicates that a transition is occurring from predominantly *direct* reaction (products once they start to separate continue to do *so* [57]) to *indirect* reaction in which subsequent "clutching" and "clouting" secondary encounters drain the incipient vibration out of the new bond into rotation and translation [58, 59], What we are seeing is the onset of statistical

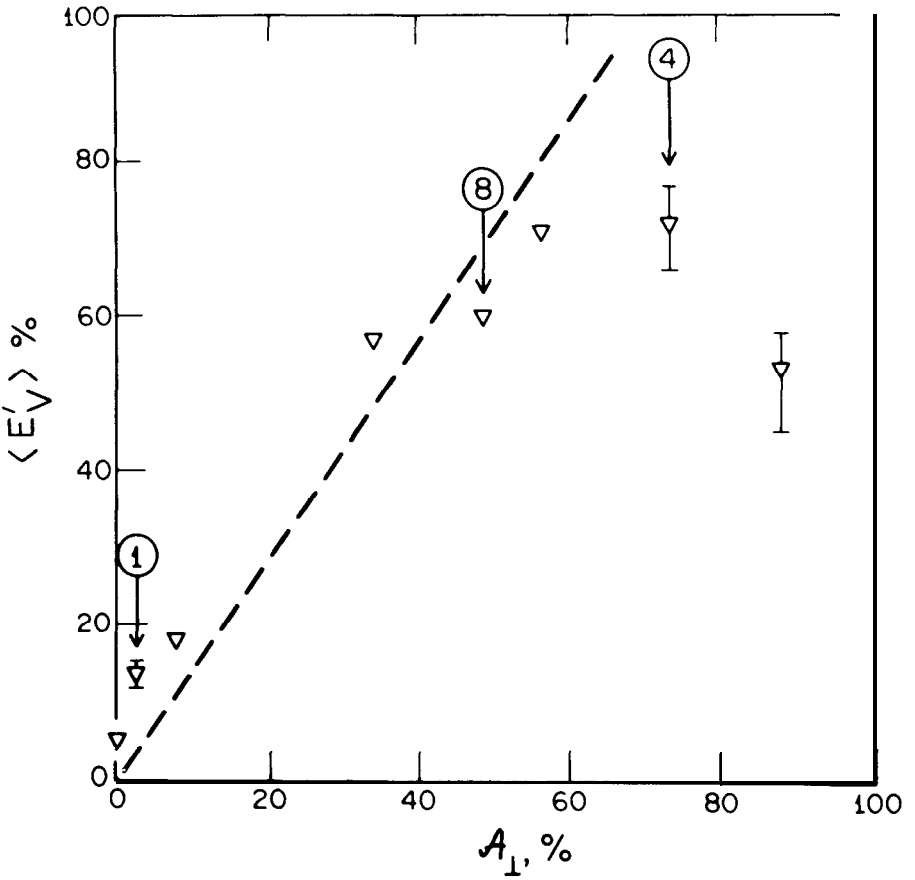

Figure 14. Mean vibrational excitation in the products of 3D L+HH reaction on 8 potential energy hypersurfaces (pes) plotted against the perpendicular attractive energy-release, AI. The collinear cuts through pes 1,8, and 4 are to be found in the previous figure. The fall-off in $\langle E'_v \rangle$ at high $A_\perp$ is due to the prevalence of secondary encounters (see text). From P.J. Kuntz et al., J. Chem. Phys. 44, 1168 (1966).

behaviour, in the limit of which product vibration will receive no more than its modest equipartition allocation.

At the other end of the scale in fig. 14, where repulsive energy-release predominates, the low vibrational excitation shown in the figure is by no means the rule; the observed vibrational excitation is strongly dependant on the chosen mass-combination. The **L+HH** mass combination shown is in fact anomalous in fulfilling the initial expectation that repulsive energy-release R (energy released along the coordinate of separation of the pes) will be inefficiently channelled into vibration. For **L+HH** the attacking atom A approaches BC rapidly up to the normal bonding separation before the repulsion is released (dynamics in which r_{AB} decreases to its equilibrium separation, r^0_{AB}, and only

then does r_{BC} increase, correspond on the pes to a rectilinear path). Since the repulsion operates on an already existent AB bond, vibrational excitation is indeed inefficient (left end of fig. 14). This behaviour is sufficiently atypical to be described as the "light-atom anomaly" [53].

For the more general case of a heavier attacking atom relative to the molecule under attack, the new bond is still extendend ($r_{AB} > r^0_{AB}$ at the time that the bulk of the repulsion is released; we can symbolise this as A- -B · C. In this case repulsion between the separating atoms B and C results in recoil of B, rather than of AB as a whole; i.e. it gives rise to efficient internal excitation of the new bond, AB.

Since the solution of the collinear equations of motion can be pictured in terms of the motion of a sliding mass across a suitably scaled and skewed representation of the pes, it is instructive to consider the characteristic path across the pes in the latter more general case. The fact that r_{AB} decreases at the same time as r_{BC} increases (we term the energy-released in this phase, "mixed"; M) means that the sliding mass, rather than following a rectilinear path, is cutting the corner of the pes. Instead, therefore, of approaching the exit valley from its head, it approaches the valley from the side; consequently it oscillates from side to side of the exit valley indicating that the new bond is vibrationally-excited.

The proportion of the energy released during corner-cutting is clearly relevant to the efficiency with which the repulsive energy is channelled into vibration. We have determined the extent of mixed energy-release, M_T, from a specimen collinear trajectory employing the appropriate mass-combination and the pes in question [10, 53, 60]. Figure 13 shows that % M_T is insignificant for **L+HH**. For other mass-combinations it is so great that the points on a plot of the type shown in fig. 14 begin at substantial <E'v>, and the region of linearity prior to the fall-off in < E'v > due to the onset of indirect dynamics becomes a very short region (see the case of the heavy attacking atom in fig. 7 of [53]).

Turning to the experimental findings of 2.1, it was evident that the moderate mean fractional conversion of reaction energy into product vibration, <f'v>, could be explained either by a highly attractive interaction leading to secondary encounters, or by a predominantly repulsive energy-release. The first of these alternatives appeared implausible since it implied a substantially broader distribution over product vibrational and also rotational states than was observed [16]. Instead the evidence favoured a strongly repulsive pes, with the light-atom anomaly explaining the markedly reduced <f'v> for $H+X_2$ as compared with $X+H_2$ or X+HY, and the lower barrier leading to a slightly increased AI in $H+Br_2$ as compared with $H+Cl_2$ (cf. the correlation noted above) accounting for the greater <f'v> observed for $H+Br_2$ than for $H+Cl_2$ [16].

The success of a strongly repulsive pes in accounting for the general form of the triangle plot for Cl+Hl → HCl + I is illustrated, by way of an example, in fig. 15 [61], which should be compared with fig. 9 above. Similar success has been obtained for the reaction $F+H_2$, → HF+H (fig. 8) above using a strongly

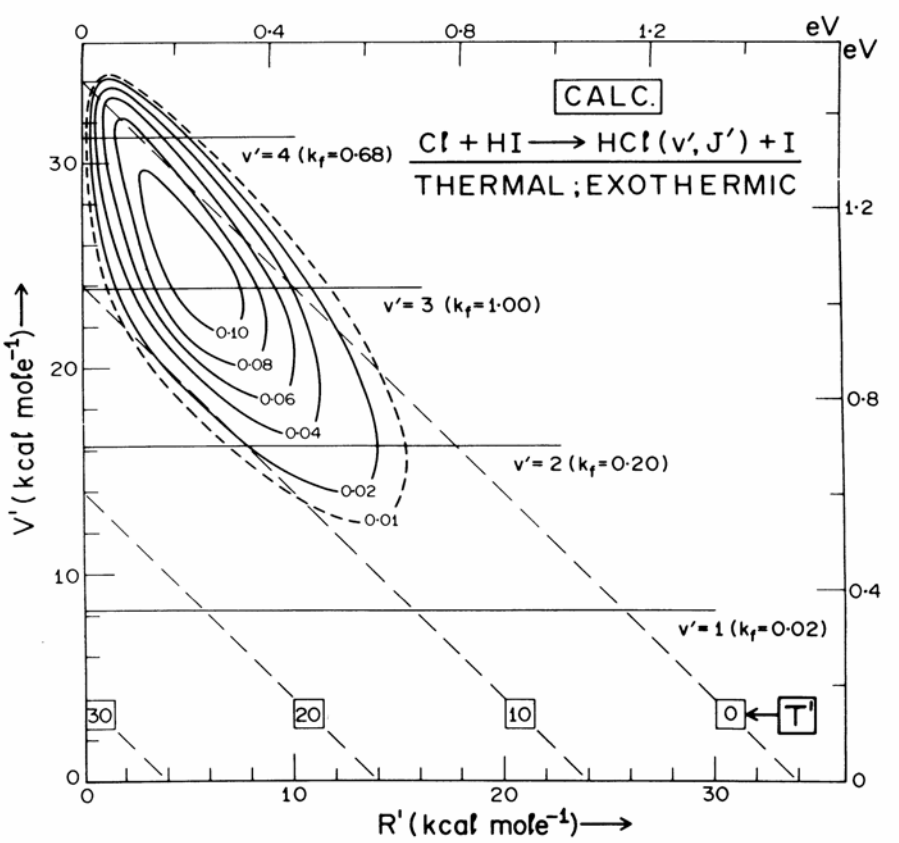

Figure 15. Computed triangle plot for the reaction Cl+HI at thermal collision energies (300K). The 3D classical trajectory method was applied to a highly repulsive pes (proposed by Anlauf et al., J. Chem. Phys. *49*, 5189 (1968)). From C.A. Parr et al., J. Chem. Phys. *58*, 5 (1973).

repulsive pes [62-64]. In this case there is now dependable evidence from *ab initio* varational treatments of FHH [65, 66] that the energy-release is indeed substantially repulsive. The success of a repulsive pes in describing **L+HH** dynamics will be demonstrated (for $H+F_2 \rightarrow HF+F$; cf. fig. 7 above) in section 3.2 below.

The discussion of the previous paragraphs as it relates to repulsive energy-release is summarized pictorially in fig. 16. Though visualisation of reaction dynamics is generally, and often adequately, based on the collinear pes to which the sliding-mass analysis applies, tests of the validity of pes' are made by 3D trajectories.

Product rotational excitation is eliminated from the picture in the collinear world. Though this is a minor constituent of the product energy, it is revealing of the dynamics. In the visualisation of fig. 16, we have included the effect of

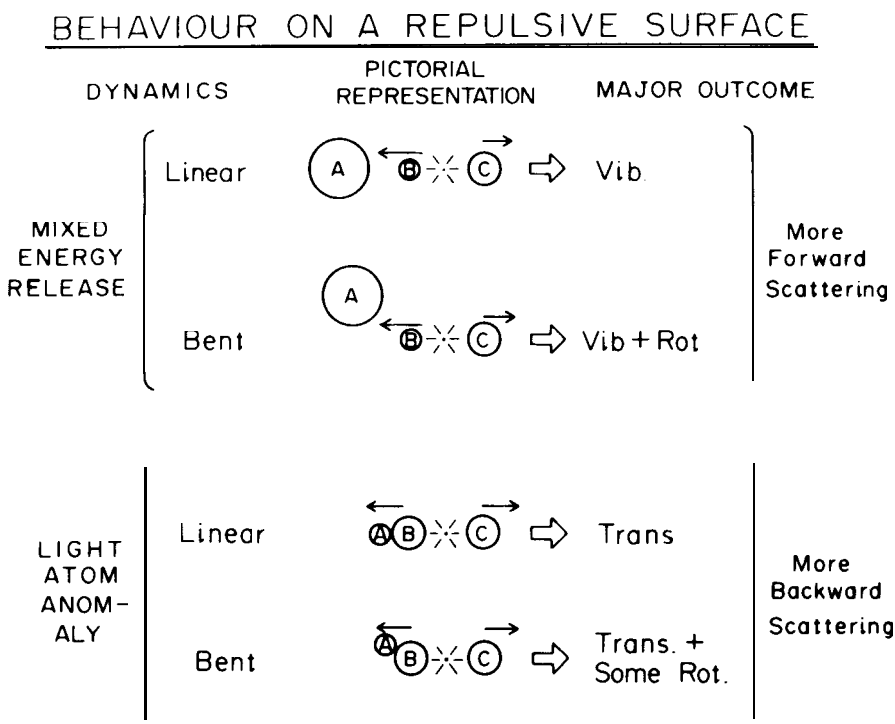

Figure 16. Pictorial representation of contrasting types of reaction dynamics on a repulsive energy surface. Type (a), "mixed energy release", is commonly observed. Type (b), termed "the light-atom anomaly", is observed if the attacking atom is very light. From J. C. Polanyi, Accounts Chem. Res *5*, 161 (1972).

repulsive energy release in bent configurations as one source of product rotation. The experimental data in the triangle plots of fig. 11 give persuasive evidence of the significance of this effect in the important reaction $F+H_2$. Product repulsion would be expected [47, 67] on the basis of momentum conservation to give rise to decreasing $\langle f'_R \rangle$ in the series FH · D > FH · H > FD · D > FD H (the dot indicated the locus of the repulsion); this is found theoretically, in 3D trajectory studies, and also experimentally. The triangle plots of fig. 11 correspond to the extremes of this range of isotopic mass-combinations; $\langle f'_R \rangle$ for the FH · D pathway substantially exceeds that for FD · H.

Qualitative pictures of the type given in fig. 16 suggest simple models of the reactive event. Several such models are indicated in fig. 17, all of which stress the role of the forces operating along the coordinate of separation of the pes. The implications of each of these models are discussed in ref. [59]. Despite their crudity simple models have the important virtue that their "moving parts" are open to inspection. Model (c), called the Simple Harmonic model, has been

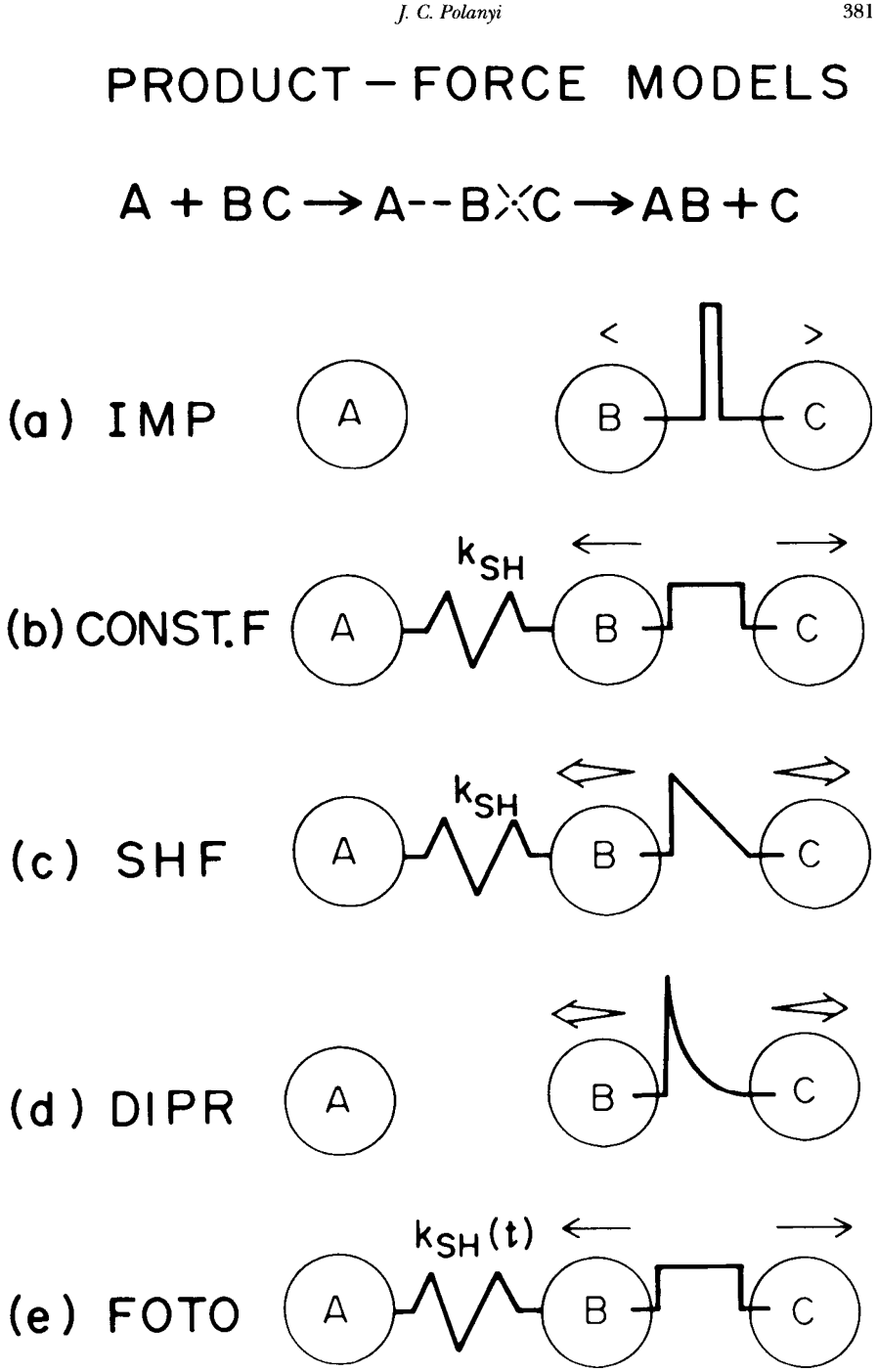

Figure 17. Five types of simple "product-force models", that interpret product energy-distributions in terms of the mode of relaxation of ABC in its retreat from the activated state→AB+C. A repulsive force is assumed to be located between the separating atoms B.C. Various assumptions are made regarding the bond A-B which is forming. Model (a) is the Impulsive model, (b) is the Constant Force model, (c) is the Simple Harmonic model, (d) is the DIPR (Direct Interaction with Product Repulsion) model, and (e) is the FOTO (Forced Oscillation in a Tightening Oscillator) model. From J.C. Polanyi, Faraday Disc. Chem. Soc., 55, 389 (1973).

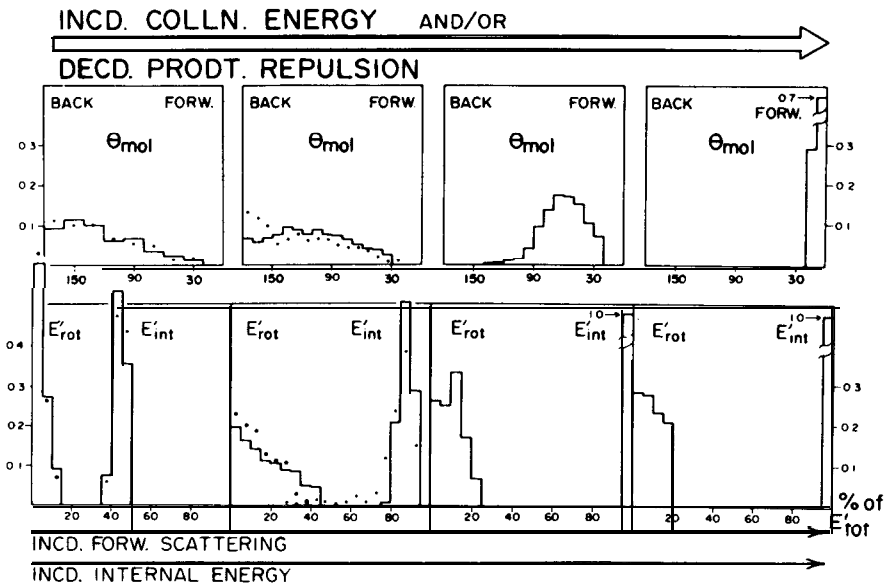

Figure 18. Effect of repulsive energy release on product angular distribution (top row) and energy distribution (bottom row; $\mathbf{E'}_{rot}$ is product rotational excitation and E'_{int} is vibration plus rotation). The solid lines show the results of 3D (three-dimensional) DIPR model calculations (masses $K+Br_2$, energy-release E'_{tot} = 53 kcal/mole). The total product repulsion used in the DIPR model calculations was decreased in four stages, from left to right in the figure, simulating decreased % *R,* implying increased % *A.* According to the DIPR model this is mathematically equivalent to increasing the reagent collision energy, hence the dual label of the arrow at the top. The consequences of these changes are summarized, qualitatively, by the arrows at the foot of the figure. The dots record the distributions obtained from 3D trajectories on potential-energy hypersurfaces with comparable partitioning of the energy-release. Adapted from P.J. Kuntz et al., J. Chem. Phys. 50, *4623* (1969).

used to improve our understanding of the mechanism of mixed energy-release, in which a repulsive force operating between particles B and C drives an oscillator joining A to B that is under tension [60]. The model shows that for a wide range of conditions mixed energy release can play a significant role in channelling product repulsion into vibration.

Model (d), the DIPR (Direct Interaction with Product Repulsion) model [68], sidesteps consideration of forces in the new bond by obtaining the product vibration, V', from E'_{tot} - (R'+T'). From the direction of recoil of atom C relative to the direction of approach of A, angular distributions can readily be generated in 3D. The model provides a simple means to expose the link between the angular distribution of reaction products and their internal excitation, as well as the connection between these two quantities and the collision energy.

Findings for the DIPR model are summarised in fig. 18 (solid lines). Reading from left to right the interactions become less repulsive (more attractive). This

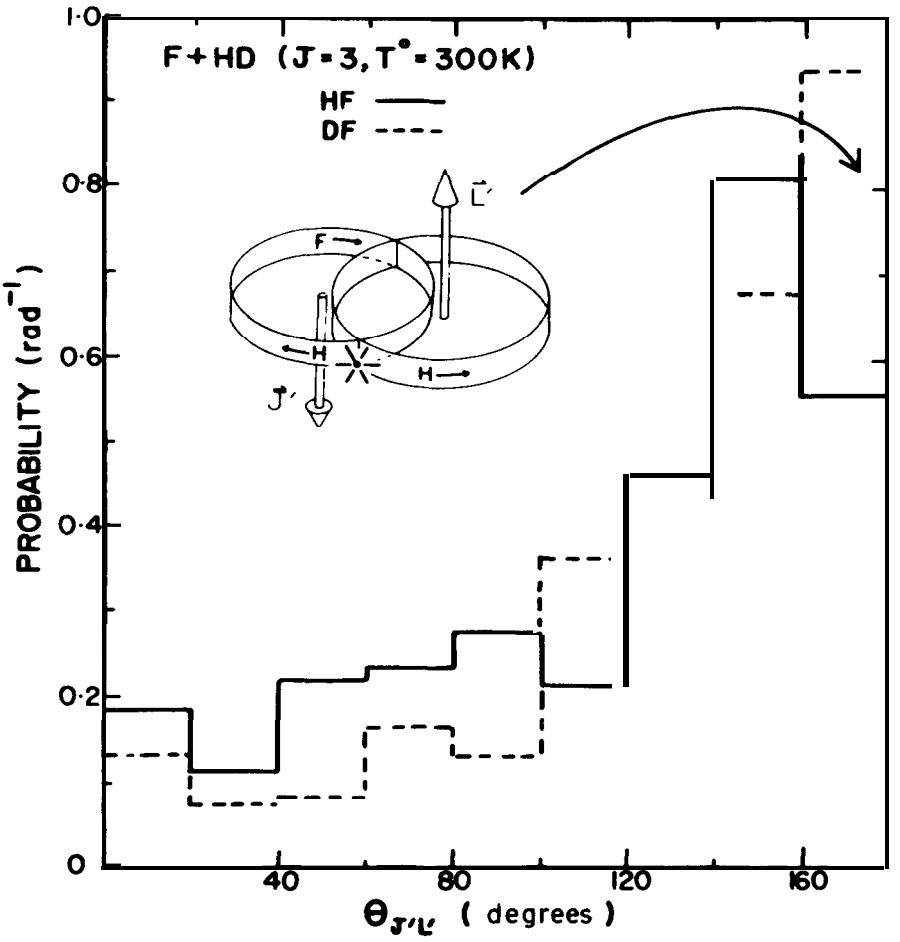

Figure 19. Computed distribution, $\theta_{J'L'}$, of the angle between the product rotational angular momentum, J', and orbital angular momentum, L', following repulsive energy-release between the products of the reaction F + HD→ HF+D (solid line) and → DF + H (broken line). At the extreme left $\theta_{J'L'} = 0$ corresponds to J' parallel to L', while at the extreme right $\theta_{J'L'} = 180°$ corresponds to the favoured outcome of J' anti-parallel to L'.

is achieved by systematically decreasing the repulsive impulse (the time integral of the force, F(t), between B and C) which alone governs the dynamics. Since a measure of IF(t) dt can be obtained by a variety of means for any actual reactive pes [59, 68], the model can be applied to cases for which the results of 3D trajectory computation are known. The agreement - see the points for the more repulsive cases in fig. 18 – is excellent, so long as the assumption of direct interaction remains valid.

The lessons that can be learned from fig. 18 are that strongly repulsive energy-release will tend to give backward scattering of the molecular product

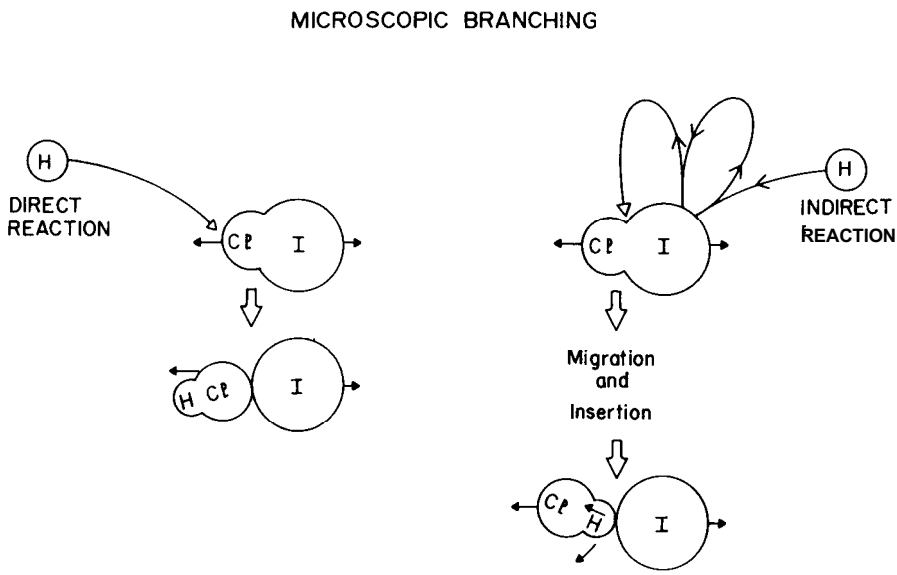

Figure 20. Pictorial representation of the alternative dynamics - direct and indirect - in the microscopic branching underlying the bimodality of product energy distribution exemplified in fig. 12. (Based on a classical trajectory study; J.C. Polanyi et al., Faraday Disc. Chem. Soc. 67, 66 (1979)).

(θ_{mol} is substantial at 180°) coupled with moderate internal excitation, E'_{int}. As the repulsion is decreased θ_{mol} shifts forward, and E'_{int} increases. The same effect can be achieved by increasing the reactant collision energy, since this too has the effect of decreasing the repulsive impulse $\int F(t)dt$.

Herschbach and co-workers have injected physical content into the DIPR model in their DIPR-DIP extension, in which the repulsive impulse is assumed to be "Distributed as In Photodissociation" [69]. The model then accounts nicely for product distributions observed in a number of reactions. More recently Zare's laboratory has shown how the DIPR approach can be used to understand the plane of rotation of new-born reaction products [70].

The FOTO (Forced Oscillation in a Tightening Oscillator) model [71], item (e) of fig. 17, gives a fuller rendition of the forces on a collinear pes; the B ·C repulsion operates on an AB oscillator whose force constant is in the process of increasing, and whose equilibrium separation, r^0_{AB}, is decreasing. The model, which has been applied to ten reactions for which experimental or theoretical data exist, is sufficiently complete to embody analogues of the "attractive", "mixed", and "repulsive" phases of energy-release.

To the extent that the rotation in a newly-formed reaction product AB originates in repulsion AB·C, the rotational motion should be coplanar with the repulsive force, and B in AB should recoil away from C. This implies that the angle between the product rotational angular momentum vector, J', and the product orbital angular momentum vector, L', should be $\theta_{J'L'} \approx 180°$.

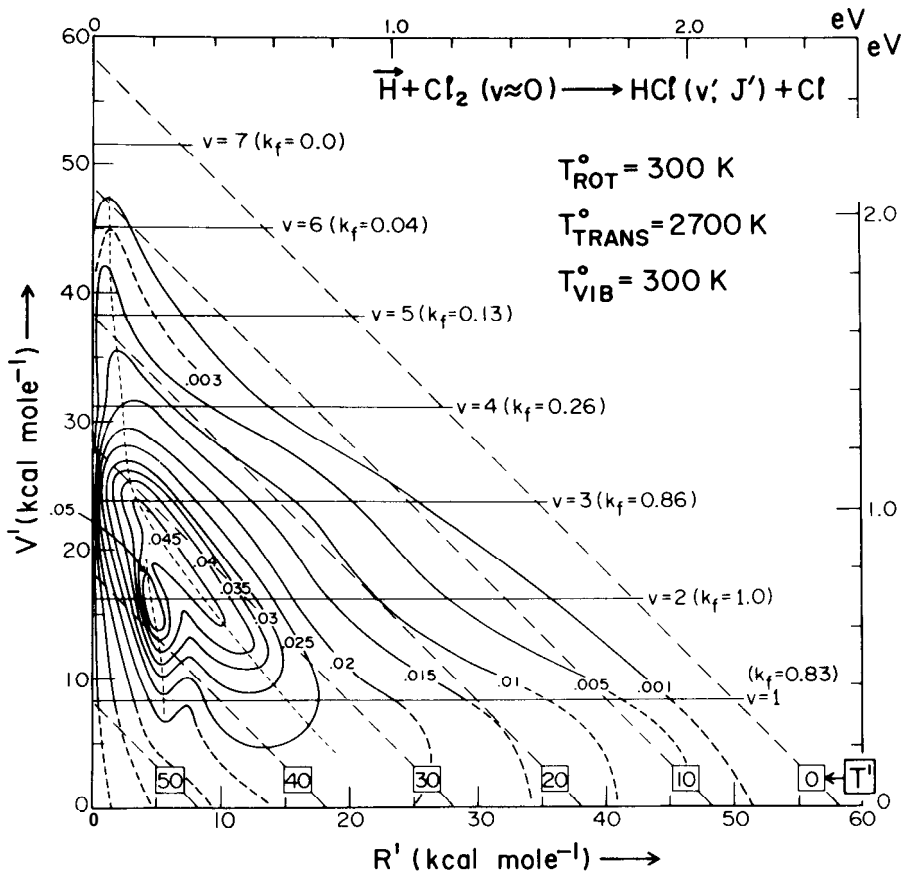

Figure 21. Effect of enhanced reagent collision energy on the product energy distribution, i.e. experimental k(V',R',T'), for $H + Cl_2(v = 0) \rightarrow HCl(v'J') + Cl$. Mean collision energy, $\langle T \rangle \approx 10.6$ kcal/mole. Compare k(V',R',T') for room temperature reaction, in fig. 6. From A.M. Ding et al., Faraday Disc. Chem. Soc., *55*, 252 (1973).

Analyses of product distributions from 3D trajectory studies [64,72] bear this out. Experimental studies of correlations between such vector attributes will add materially to the mosaic from which our picture of reaction dynamics is composed.

The richer the detail in the rate constants k(V', R', T'), the clearer the message. The striking bimodality in the product energy-distribution from H + CII ↦HCI(v', J') + I recorded in fig. 12 can be ascribed to "microscopic branching"; two patterns of molecular dynamics result in the formation of the same reaction product (HCI in this example). The dynamics have been explored in 3D. They are shown schematically in fig 20. In the case of H + CII the migratory *microscopic* pathway (at the right of fig. 20) is thought to dominate. This is for the same reason that *macroscopic* branching favours formation of HI rather than HCl, namely the existence of a smaller energy barrier for approach

from the I end of ICl (see [73] for the greater stability of ClIH than HClI). In collisions of H with the I end of ICl that fails to yield HI, the H atom can migrate to the Cl end of the molecule to yield highly internally-excited HCl. The HCl product with low internal excitation comes from H that have reacted directly at the Cl end of ClI. Since the barrier to this mode of reaction is higher, the yield (at normal reagent energies) is lower. It is evident that the relative yields of HCl and HI in *macroscopic* branching are linked to the yields of low E'_{int} and high E'_{int} HCl by way of *microscopic* branching.

Microscopic branching is thought to constitute more than merely an interesting curiosity, since it can contribute to the dynamics in any case where macroscopic branching is possible - a large class of reactions. As would be expected, the importance of microscopic branching, in common with macroscopic branching, depends sensitively on the reagent energy [49, 50, 74].

3. CHANNELLING REAGENT ENERGY INTO PRODUCTS

3.1 Experiment

In the experiments that will now be briefly described reagent translational, vibrational, and rotational energies were altered by simple means in order to explore the effect on the product energy-distribution. To increase the collision energy we formed the atomic reagent (Cl for Cl + Hl [75], F for F + HCl [50] or F + H_2 [50,67], and H for H + Cl_2 [50]) by pyrolysis, rather than using room temperature atoms as in the work described in the previous section. The effect is shown for H + Cl_2 in the triangle plot of fig. 2 1. Comparison with the earlier 300K triangle plot (fig. 6) shows marked changes. The *additional* reagent translation, ΔT, in excess of the barrier to reaction, has been channelled principally into additional product translation.

A second repository for this additional reagent energy was product rotation. (It was interesting to observe in both Cl + HI [75] and H + Cl_2 [50] that this enhanced product rotation was associated with the appearance of a second maximum in the product rotational distribution, $k(J')_{v1}$, as if enhanced collision energy had led to *induced microscopic branching).* The general finding regarding the disposition of additional reagent translation could be summarised as,

$$\Delta T \rightarrow \Delta T' + \Delta R' \qquad (4)$$

This describes the average behaviour; the breadth of the product energy distribution increased markedly over V′, R′, and T′.

By heating the molecular species under attack and recording the change in product energy distribution (see fig. 22), we found evidence of a similiar adiabaticity, on the average, in regard to the conversion of reagent vibration into product excitation,

$$\Delta V \rightarrow \Delta V' \qquad (5)$$

where the symbol Δ denotes energy in excess of that required for barrier crossing. As before, the breadths of the product energy distributions increased, that over V′ appearing to be bimodal.

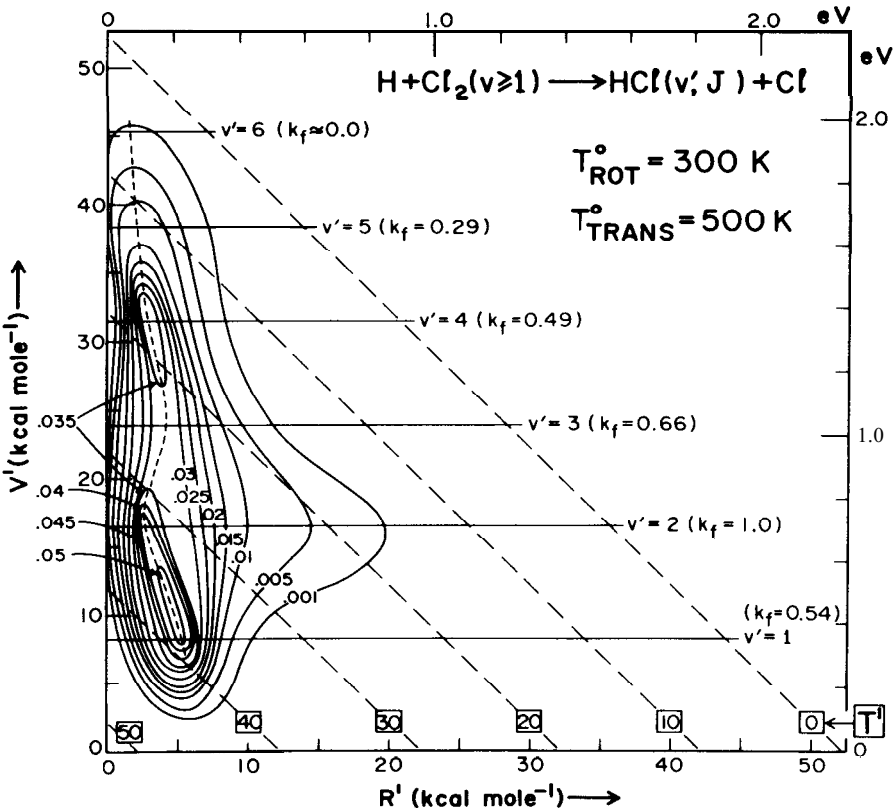

Figure 22. Effect of enhanced reagent internal energy on the product energy distribution, i.e., experimental k(V',R',T'), for $H + Cl_2(v \geq 1) \rightarrow HCl(v', J') + Cl$. This result is approximate since it was obtained by subtracting the detailed rate constants for $H + Cl_2(v \approx 0) \rightarrow HCl + Cl$ from $H + Cl_2(v \geq 0) \rightarrow HCl + Cl$. Mean vibrational energy, $\langle V \rangle \approx 3.3$ kcal/mole. Compare with fig. 6. From A.M.G. Ding et al, Faraday Disc. Chem. Soc. *55*, 252 (1973).

A more stringent test of this tendency toward vibrational adiabaticity was obtained using the method of ir chemiluminescence depletion (CD; section 4.1 below) and ir emission. Vibrationally excited reagent, OH(v), was formed in a selected "pre-reaction". Pulses of a further reagent - Cl in the present case - were introduced, and a record was made of the depletion of chemiluminescence (at the pulsing frequency) in OH(v), as well as of the appearance of chemiluminescence in reaction product HCl(v'). The reaction responsible for both emissions was

$$Cl + OH(v) \rightarrow HCl(v') + 0 \qquad (6)$$

Using two different pre-reactions (see caption fig. 23) the reagent vibrational energy could be given mean values of $\langle V \rangle = 72.1$ kcal/mole or 20.5 kcal/mole. For these high vibrational energies over 90 % of the reagent vibration

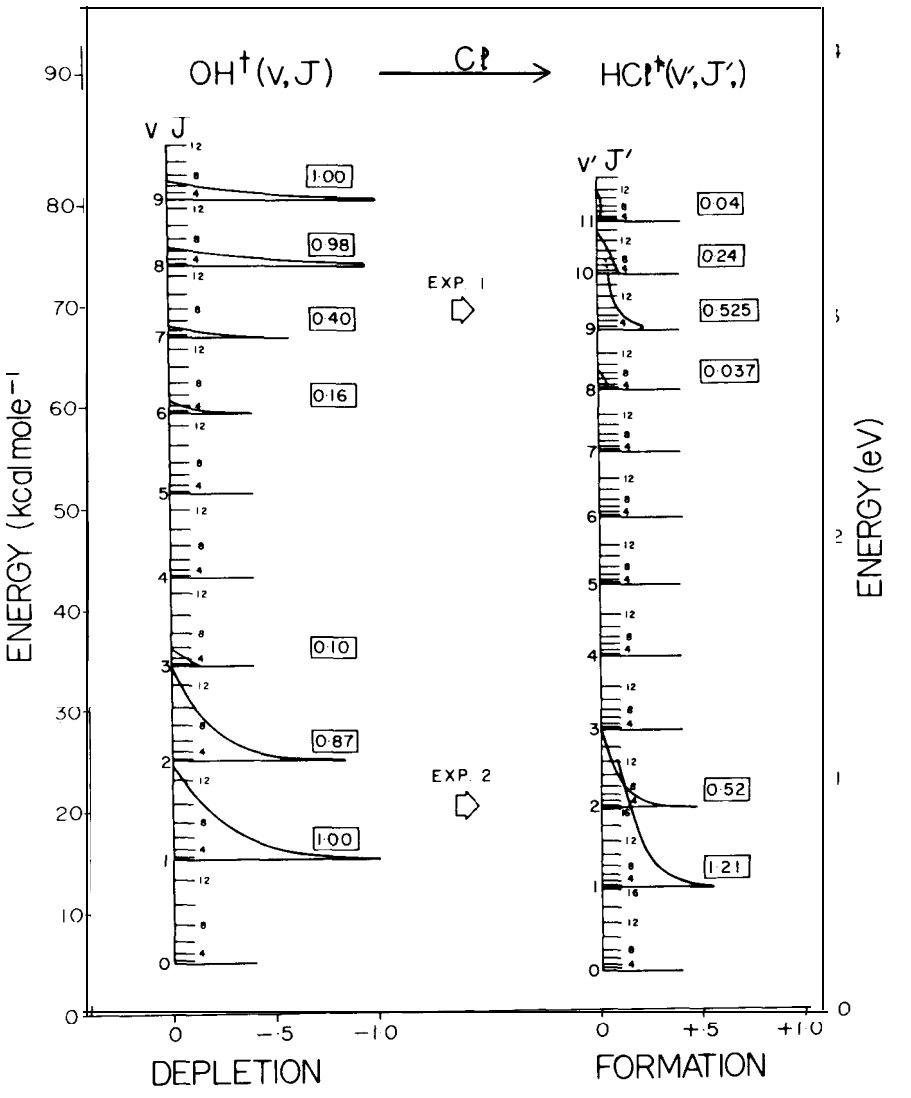

Figure 23. Experimental evidence for the conversion of high reagent vibrational excitation into the corresponding degree of freedom of the product in the reaction Cl + OH(vJ) → HCl(v'J') + O. The curves at the left show the *decrease* in population of each OH vibrotational level resulting from the introduction of Cl atoms; the curves at the right were taken from a concurrent record of the amount of HCl formed in each vibrotational level. In experiment 1 (top of figure), the OH was formed in v = 6-9 by the pre-reaction H + O_3. In experiment 2 (lower part of figure), the OH was formed in v = 1-3 by the pre-reaction H + NO_2. The numbers in the boxes at the left give the relative fractional depletions of each OH v-level (summed over J), and those at the right give the corresponding information for the product HCl. From B.A. Blackwell et al., Chem. Phys. 24, 25 (1977).

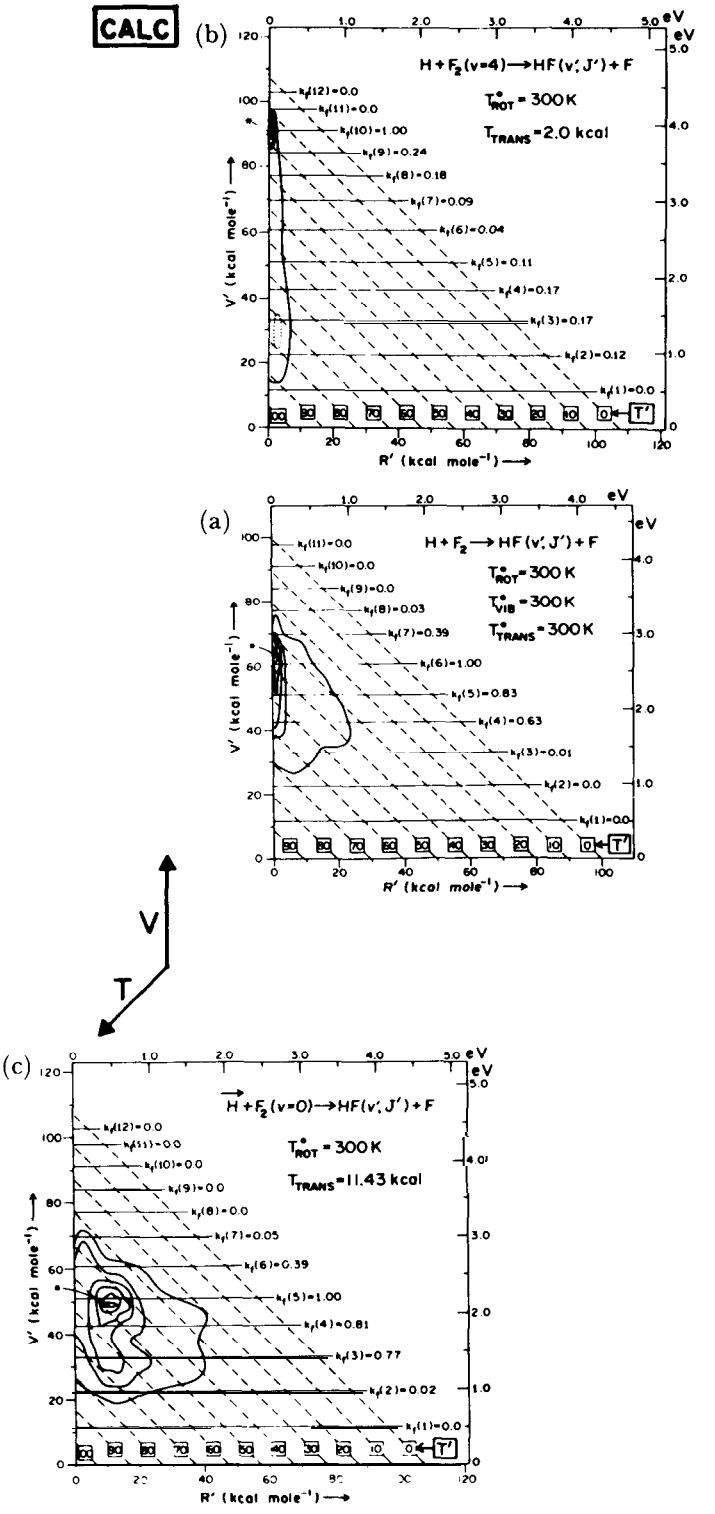

Figure 24. Computed triangle plots for the H + F_2 reaction. In (a) the reagents were Monte Carlo selected from a 300K Boltzmann distribution. In (b) the F_2 reagent vibrational excitation, V, was increased to v = 4 (reagent collision energy 2.0 kcal/mole), and in (c) the reagent relative translational energy, T, was increased to 11.43 kcal/mole (reagent vibrational energy corresponded to v = 0). From J.C. Polanyi et al., Chem. Phys, 9, 403 (1975).

was found to be channelled into product vibration. Once again $\Delta V \rightarrow \Delta V'$ [76].

Evidence regarding the fate of reagent rotation was more fragmentary, coming from studies of the reaction F + $H_2(J)$ with J varied systematically from $0 \rightarrow 1 \rightarrow 2$ [77]. A small but significant decrease was observed in the fraction of the total energy entering product vibration when $J = 0 \rightarrow 1$, followed by an increase in this fraction as $J = 1 \rightarrow 2$. This finding was in accord with an earlier less detailed study by Coombe and Pimentel [78]. As is often the case at present with the effects of reagent rotation (see 4.2 below), detailed understanding is lacking.

3.2 *Theory*

The nature and the origins of the approximate adiabaticity relations (4) and (5) have been discussed in a number of places [49,50,54,61,67,79-82]. The success of the 3D classical trajectory method in describing the types of change in detailed rate constant observed experimentally (see figs. 21 and 22) can be judged from fig. 24 [81]. This figure shows a computed triangle plot for the 300K H + $F_2 \rightarrow$ HF(v'J') + F reaction at the centre (see fig. 7 for the experimental counterpart), and the predictions for enhanced reagent translation (ref. [82] fig. 3 has the experimental counterpart) and vibration, below and above respectively. It is evident from inspection of fig. 24 that $\Delta T \rightarrow AT' + AR'$, and $\Delta V \rightarrow \Delta V'$. In addition the increased breadths of product energy distributions over T' and R' in the former case, and over V' in the latter are apparent, as also is the bimodality over V' resulting from enhanced V. (See [50] for comparable trajectory studies using parameters chosen for H + Cl_2).

The origin of this adiabaticity is evident from an inspection of trajectories with and without the additional reagent energy. The effect of enhanced translation is to shift the characteristic pathway across the collinear pes (used as a diagnostic of 3D behaviour) toward more-compressed configurations - the sliding mass impelled by its enhanced momentum along r_{AB} caroms into the corner of the pes in the region of ① in fig. 25. The compressed intermediate $A \cdot B \cdot C$ if collinear then flies apart to give translation in AB + C, and if bent to give enhanced rotation in AB. For enhanced reagent vibration the most common paths to product are shifted to the region ② in fig. 25; the effect is to favour a more stretched intermediate A-B-C that pulls together along r_{AB} to give AB($v \geqslant 0$) + C. The opposite phase of vibration to that pictured in fig. 25, drives the intermediate into region ① giving rise to the low V' peak in the product distribution. Since energy released along r_{BC} has been characterised as repulsive and that along r_{AB} as attractive, we have termed these changes in dynamics *induced repulsive energy-release* in the first case, and *induced attractive energy-release* in the second. For a strongly exothermic reaction such as H + F_2 (fig. 24), these shifts affect not only the channelling of the additional reagent energy, but also the channelling of the exothermicity into product excitation, so that $(\Delta T' + \Delta R')/\Delta T$ and $\Delta V'/\Delta V$ exceed unity [81].

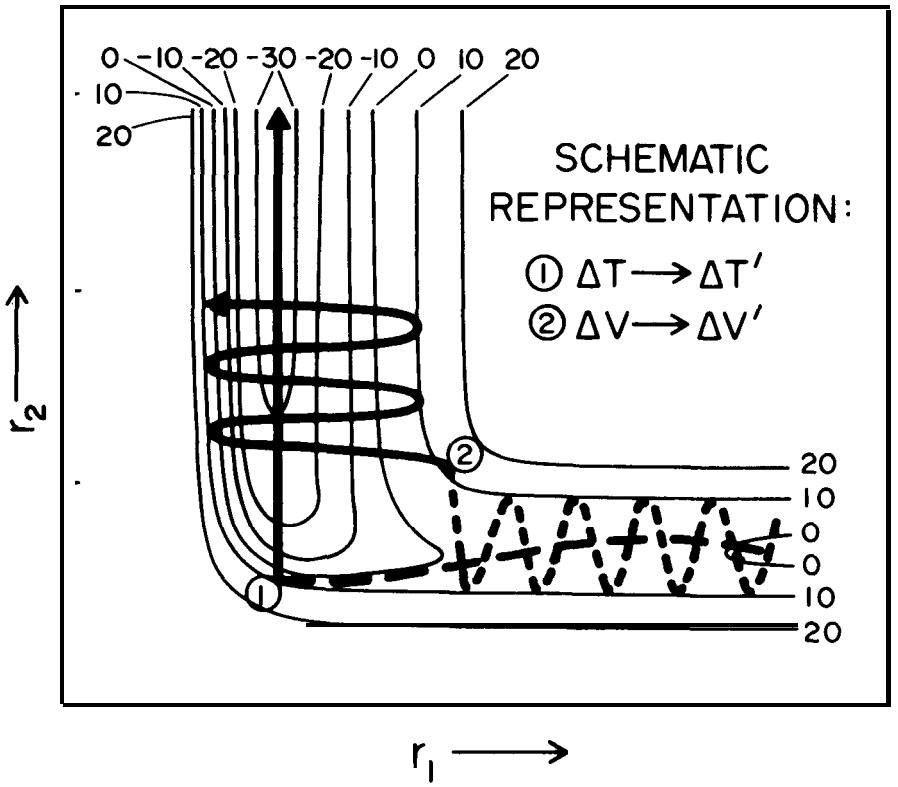

Figure 25. Schematic representation (on a typical collinear exothermic pes) of the mechanism (1) by which "additional" reagent translation ($\Delta T \gg E_c$, where E_c is the barrier height) is channelled into "additional" product translation ($\Delta T'$), and also (2) the mechanism by which "additional" reagent vibration ($\Delta V \gg E_c$) becomes "additional" product vibration ($\Delta V'$). (These are not actual trajectories since they show neither the exothermic energy-release nor the effect on that energy-release of changing reagent energy; the intention, which is artificial, is to show the effect of ΔT and ΔV in isolation). From A.M.G. Ding et al., Faraday Disc. Chem. Soc. *55, 252* (1973).

4. SURMOUNTING THE ENERGY BARRIER

4.1 Experiment

The most detailed information regarding the relative efficiency of various types of reagent motions in surmounting an energy barrier, comes from the application of microscopic reversibility to detailed rate constants for forward reaction, kf(V',R',T')[83]. Detailed rate constants for the reverse reaction obtained in this way, k_r(V',R',T'), are recorded in the triangle plot of fig. 26, where V',R',T', are now the vibrational, rotational and translational energies of the *reagents* for the endothermic reaction HF(v'J') + H → F + H_2[84]. The total energy available for distribution is fixed by the nature of the experiment, being equal to the energy made available by the forward exothermic reaction; 34.7 kcal/mole in the case illustrated. This approach has been tested numerically by applying it to a case where k_r(V',R',T') could be obtained directly from 3D

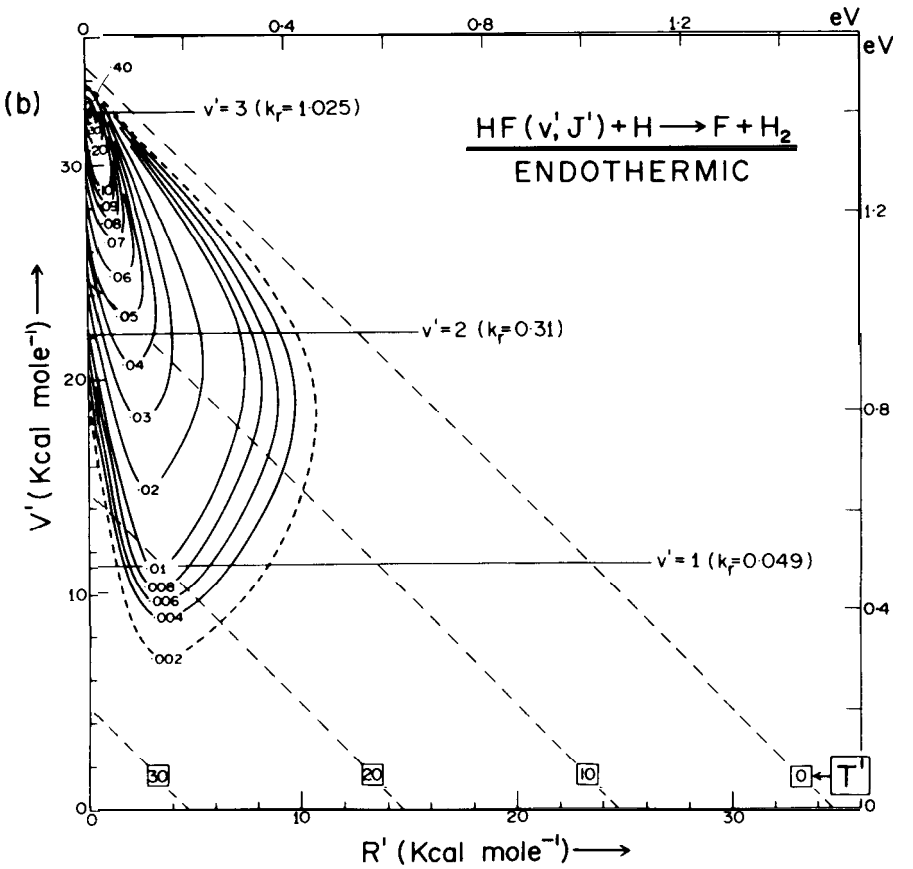

Figure 26. Contours represent values of *reagent* vibrational, rotational, and translational energies for the endothermic reaction HF(v'J') + H → F + H_2 which correspond to equal $k_r(\equiv k_{endo})$. The data were obtained by application of microscopic reversibility to the $k_f(\equiv k_{exo})$ given in fig. 8. From J.C. Polanyi and D.C Tardy, J. Chem. Phys. 51, 5717 (1969).

trajectories or by application of microscopic reversibility; the procedures agreed with one another to approx. 10% [85].

Inspection of fig. 26 indicates that a redistribution of 30 kcal/mole from T' into V' has the dramatic effect of increasing by ~ 10^3x the rate of reaction in the endothermic direction [58,84]. Endothermic triangle plots of this type are to be found in, for example, references [67,83,84]. In a few cases, in other laboratories, direct measurement has been made of the relative efficiency of vibration and translation in surmounting an energy barrier ([86-88]); in one of these cases [88] the barrier corresponded to "substantially" [67] endothermic reaction: the reaction was HE (v') + K ⟶ H + KF (17 kcal/mole endothermic) and the effect of transferring 11 kcal/mole from reagent translation to vibration was to give > 10^2x increase in reaction rate.

The infrared "chemiluminescence depletion" (CD) method, already alluded

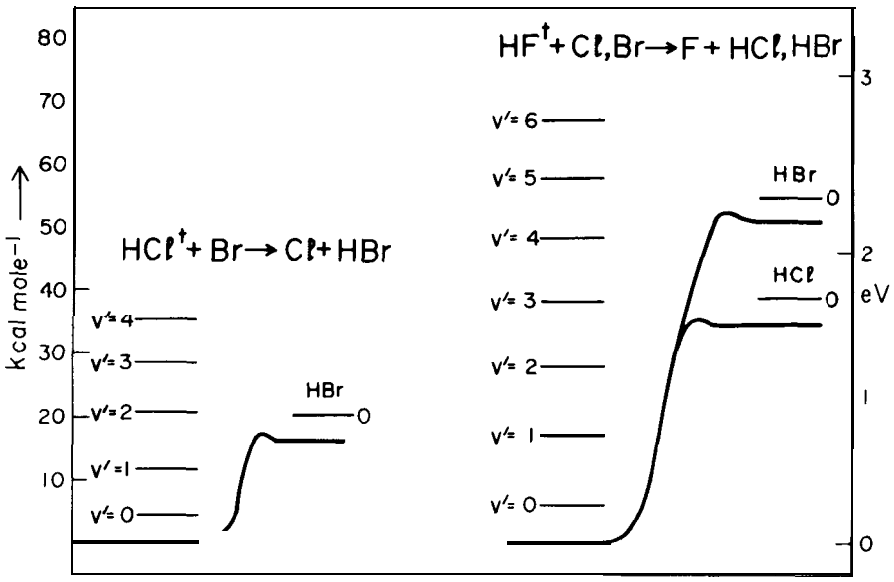

Figure 27. Endothermicities of three reactions HX + Y → X + HY; showing kcal/mole at left, eV at right, and the vibrational spacing of the relevant HX within the figure. Energy profiles are schematic. From D.J. Douglas et al., Chem. Phys. *13*, 15 (1976).

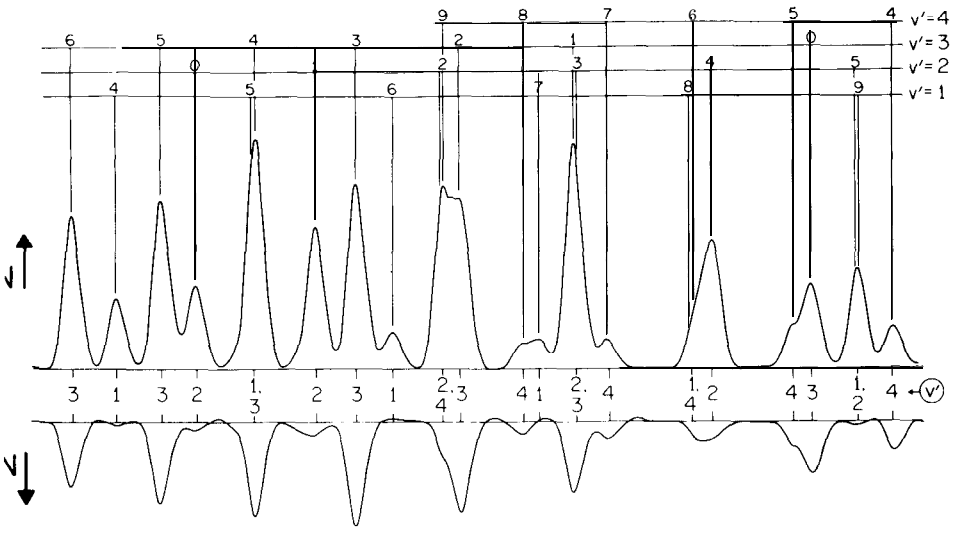

Figure 28. A portion (one fifth) of the spectrum recorded in an ir chemiluminescence depletion (CD) study of the endothermic reaction HCl(v' = 1-4) + Br → Cl + HBr. At the top (labelled N) is the emission from the HCl(v' = l-4) formed in a pre-raction. Below (ΔN) is the concurrent record of the depletion, due to pulses of Br (trace enlarged 2.5x). The fraction $\Delta N(v')/N(v') > 0$ for $v' \geq 2$. (Excursions of ΔN above the baseline can be identified with product emission (HBr(v=1,2) rather than reagent depletion.) From DJ. Douglas et al., J. Chem. Phys.. 59, 6679 (1973).

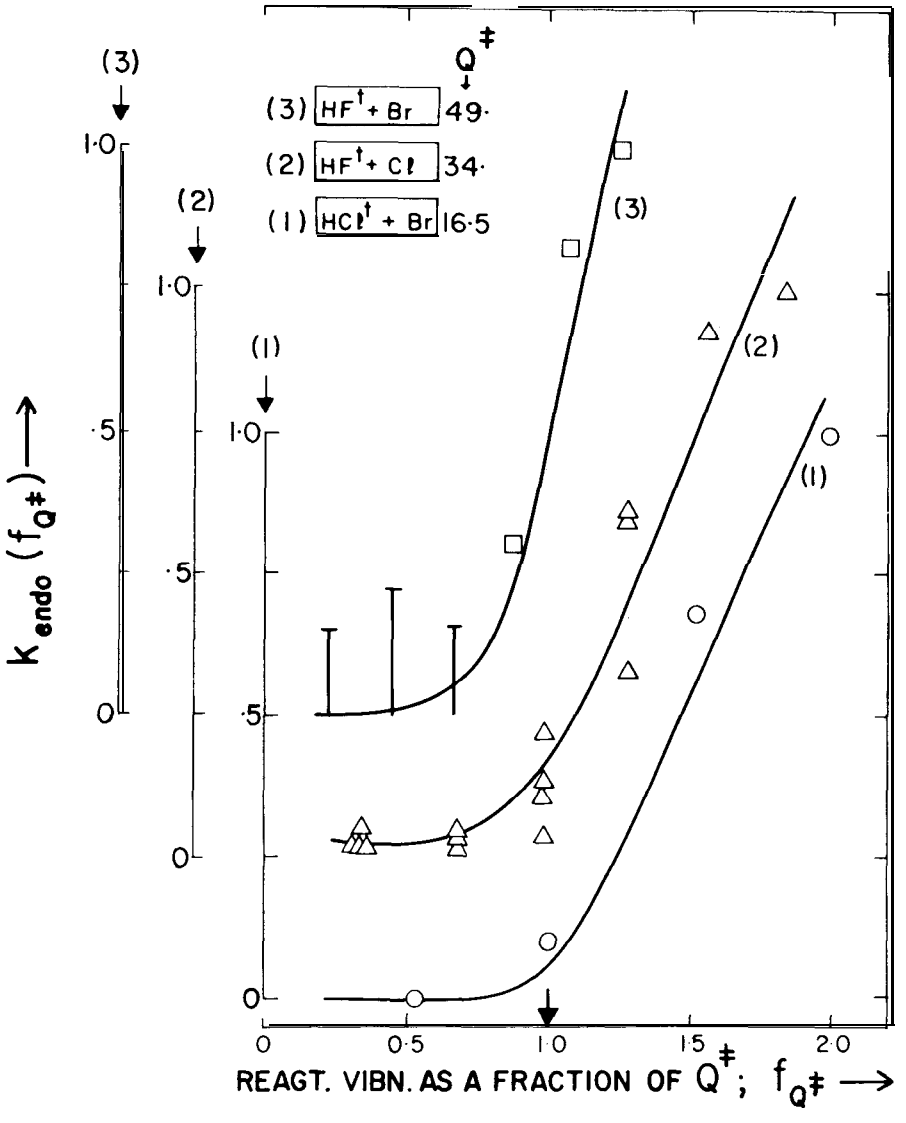

Figure 29. Endothermic rate constant $k_{endo}(f_{Q\ddagger})$; $f_{Q\ddagger}$ is the reagent vibrational energy expressed as a fraction of the endothermicity Q‡ for reactions (1)–(3). From D.J. Douglas et al., Chem. Phys. *13*, 15 (1976).

to in section 3.1, was used to obtain a measure of the efficiency of a high degree of vibrational excitation in promoting endothermic reaction. In contrast to the microscopic reversibility procedure outlined above, by CD the vibrational energy could be varied independently of the collision energy and could be made much larger than the endothermic barrier height. The energies of one family of endothermic reactions investigated in this fashion is shown in fig. 27; $HX^\dagger + Y \rightarrow X + HY$, where X = Cl or F, Y = Br or Cl and the dagger indi-

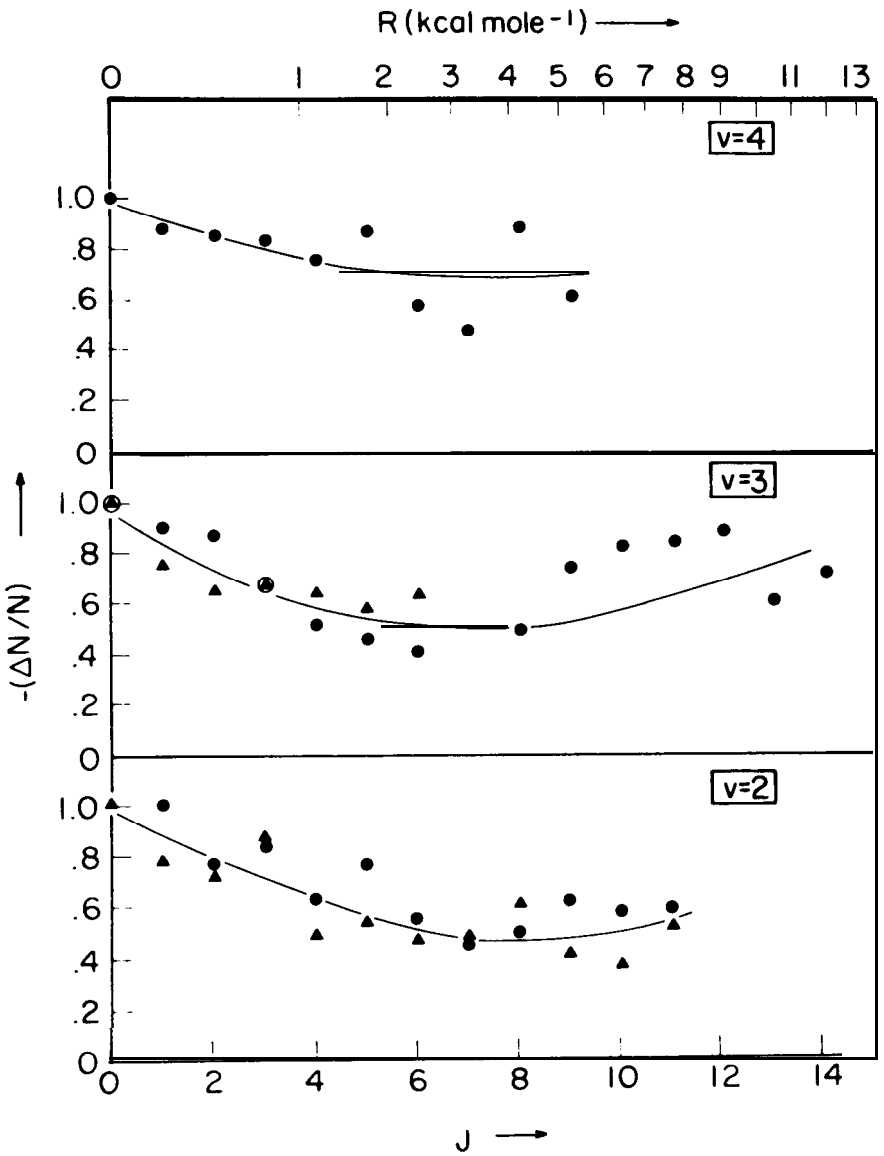

Figure 30. Fractional depletions of individual J states of v = 2-4 in a CD study of the endothermic reaction HF† + Na. From B.A. Blackwell et al., Chem. Phys. 30, 299 (1978).

cates vibrational excitation [89]. An analogous study has been made of the endothermic reactions HX† + Na → H + NaX, X = Cl,F[90]. For CD experiments, the vibrationally excited reagent HX† was formed in a variety of prereactions or in a variety of partially-relaxed vibrational distributions from single prereaction. The atomic reagent, Y or Na, was pulsed and a concurrent record was made of the ir chemiluminescence from HX† (cw) and of the

depletion (CD was measured on an amplifier locked to the pulsing frequency of the Y or Na beam).

A small portion of the concurrent spectral traces from an experiment on HCl(v'J') + Br [89] is given in fig. 28. The fractional depletions (aN(v'J')/N(v'J')), which should be independent of N(v'J'), gave a measure of the endothermic rate constant, $k_{endo}(v'J')$. Values of $k_{endo}(v')$ (summed over J') are shown plotted against the reagent energy expressed as a fraction of the endothermic barrier height, Q # in fig. 29 [89]. The onset of k_{endo} is marked for each reaction by a threshold at the expected Q # (Q#= 16.5, 34 and 49 kcal/mole for the reactions indicated in the figure). The reagent translation energy corresponded to 300K; it follows that approx. 95% of the reagent energy was present as vibration. Calibrations showed that the reactive cross section for high v', exceeded $1Å^2$, i.e. the collision efficiencies for reaction approached ~0.1. With an analogous preponderance of vibration in the reagents of $HX\dagger+Na$, the collision efficiences approached unity [90]. We conclude that vibrational excitation is highly efficient in carrying these reactions over their endothermic energy-barriers.

The CD approach was also used to map out the dependence of reaction rate on reagent rotational excitation. The results shown in fig. 30 for the endothermic processes $HX(J)_v+Na\rightarrow H+NaX$ are typical of the findings from CD. Comparable results were obtained (by a cruder approach) for the exothermic reaction $F+HCl(J)_v$ [50]. There is an initial decline in reaction probability with increasing J, followed by a rise in reaction probability. Similar behaviour has been noted in crossed beam experiments [92,93]. Nonetheless our knowledge of k(J) leaves much to be desired.

4.1 *Theory*

We have found it useful and revealing to link the preferred type of reagent energy-distribution to the location of the energy-barrier on the collinear pes (termed a "diagnostic cut" through the full hypersurface which gives the 3D dynamics). In the first approximation we have looked for a correlation between the dynamics of barrier-crossing and the location of the barrier crest relative to the point at which the entry and exit valleys of the pes may be said to meet on the collinear pes, namely the equal-stretch configuration, ϱ^*, for which $r_{AB}-r^o_{AB}=r_{BC}-r^o_{BC}$ [94]. Duff and Truhlar [95] have examined an alternative definition of the point where entry and exit valleys meet, namely the point of maximum curvature, C*, of the minimum-energy path across the collinear pes (a concept pre-figure in work of Hofacker and Levine [96]). Since the two bonds change length with minimum expenditure of energy at their maximum extension, it is understandable that $\varrho^*\approx C^*$ [97].

Figure 31 shows the dynamics characteristic of equal masses reacting across a pes with "early barrier" (surface I), at the left, and "late barrier" (surface II) at the right [94]. The barrier crest was located approx. 0.03 Å ahead of ϱ^* on surface I, and 0.03 Å beyond ϱ on II (these surfaces are designated + I and + II in fig. 31. since the labels -I and -II were used for potential hollows similarly

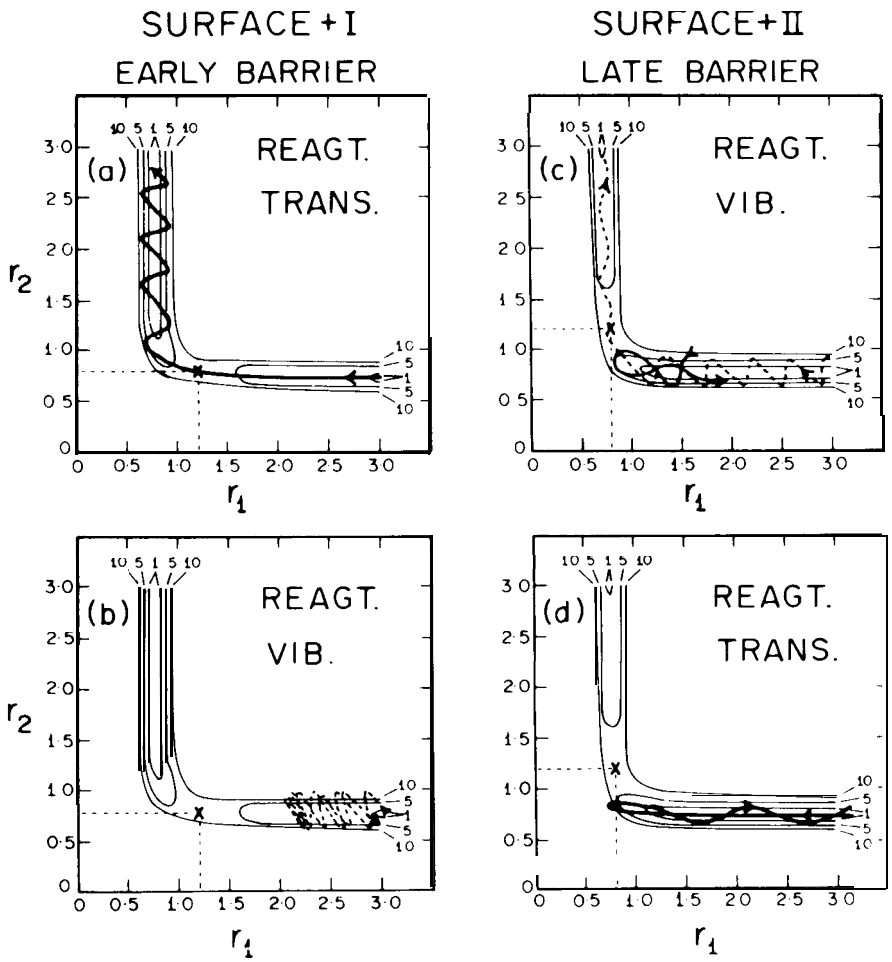

Figure 31. At the left (a) and (b) show specimen trajectories with (a) largely reagent translation (T = 9,V = 0) and (b) largely reagent vibration (T = 1.5 and V = 14.5) on an "early barrier" surface, i. e., type I. At the right (c) and (d) show trajectories with (c) largely reagent vibration (T = 1.5 and V = 7.5) and (d) largely reagent translation (T= 16.0, V = 0). All energies are kcal/mole; reagent vibration relative to E(v=0). Three equal masses, $m_A = m_B = m_C$. Positive and negative vibrational phases in solid and broken lines. Barrier heights on both surfaces I and II are 7 kcal/mole; contours are labelled in kcal/mole. From J.C. Polanyi and W H. Wong, J. Chem. Phys. *51,* 1439 (1969).

displaced from ϱ^* [58]). The effect of these displacements of the barrier crest upon the preferred mode of motion in the reagents was dramatic. As illustrated in fig. 32, on surface I a reagent translational energy only slightly in excess of the 7 kcal/mole barrier height gave a calculable cross section, whereas a reagent vibrational energy double the barrier height gave a reactive cross section too small to be computed in our study. The converse behaviour is seen

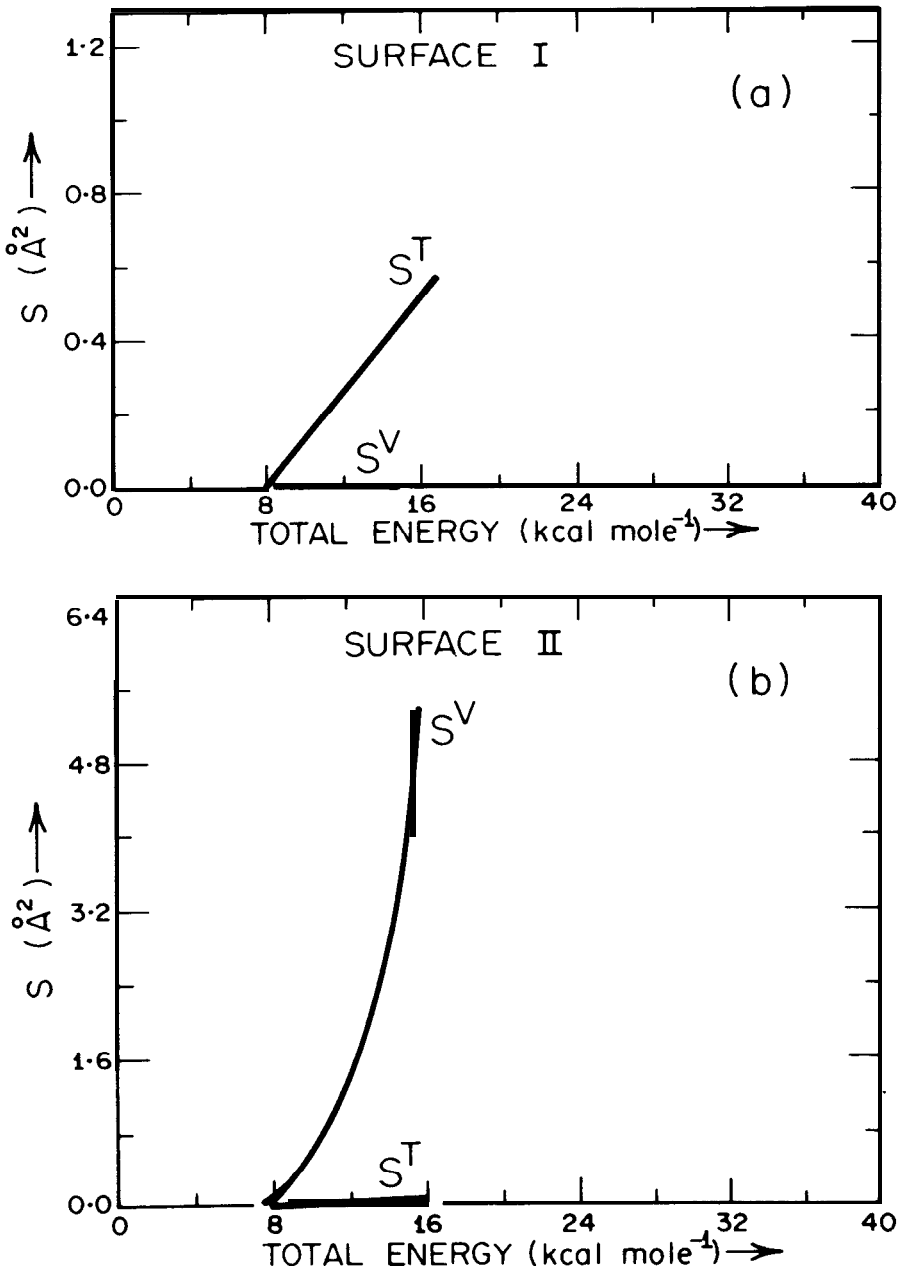

Figure 32. (a) Reactive cross-sections S^T (reagent energy in translation) S^V (reagent energy in vibration, + 1.5 kcal/mole of translation) on the "early barrier" surface depicted at the left of fig. 31. (b) Reactive cross-sections S^T and S^V on the "late barrier" surface shown at the right of fig. 31. Three equal masses. From J.C. Polanyi and W.H. Wong, J. Chem. Phys., *51,* 1439 (1969).

to apply to surface II, fig. 32; reagent vibrational energy (with a small amount of translation to bring the reagents together) was highly effective in giving reaction, whereas translation was without effect.

As we have remarked, these correlations are of more than empirical value; by focussing attention on certain simple attributes of the pes, we can shed light upon dominant features of the dynamics. In terms of the dynamics of the reaction A + BC the correlations noted in the preceding paragraph reduce to the proposition that a barrier predominantly along the coordinate of approach, r_{AB}, is best traversed by motion in that same coordinate, namely reagent translation, whereas a barrier predominantly along the coordinate of separation, r_{BC}, is best traversed by motion in that coordinate, i.e., vibration in the bond under attack. The trajectories in fig. 31 (obtained by solution of the equatons of motion, but capable of being pictured as the motion of a sliding mass across the pes) illustrate this; the reactive cases are (a) and (c) (early and late barriers), the nonreactive are (b) and (d) (early and late barriers once more). The effect illustrated is sufficiently striking that it may also have relevance to the dynamics of reactions involving many atoms (cf. [99]), provided that these occur by a direct pathway.

The interest of these correlations is greatly increased if we can link the form of the pes to the nature of the chemical reaction. Though unrecognised by reaction dynamicists, Hammond's postulate [100] that for endothermic reactions the transition state resembles reaction products might have pointed the way to the desired connection.

Instead a systematic study of a considerable number of exchange reactions $A + BC \rightarrow AB + C$ in terms of both the London, Eyring, Polanyi, Sato (LEPS), and the Bond-Energy Bond-Order (BEBO) methods led to the conclusion that for substantially exothermic reactions the barrier-crest is located in the entrance valley ("early barrier") of the pes, and for substantially endothermic reactions it is in the exit valley ("late barrier") [55]. From this, and the dynamical study of early and late barriers, it followed (as previously surmised [101]) that the favoured degree of freedom for barrier-crossing in substantially exothermic reactions would be translation, whereas reagent vibration would be most effective in giving rise to substantially endothermic reaction. (In the BEBO approximation "substantially" has the meaning $\geqslant 10$ kcal/mole [67]).

Behaviour of the type illustrated in fig. 32(a), computed for the well-studied exothermic reaction $F + H_2 \rightarrow HF + H$ is shown in ref. [64]. Behaviour of the type illustrate in fig. 32(b) is in accord with the evidence of section 4.1 above. There is, nonetheless, a clear need for comparisons of what we have termed (fig. 32) S^T with S^V for a range of reactions, and within related series of reactions.

If barrier location is to be made to any degree a quantitative index of the relative efficacy of translation and vibration in bring about barrier-crossing, the location of the barrier must be considered as it appears on a surface skewed and scaled for the appropriate masses m_A, m_B, and m_C, so that a sliding mass will correctly solve the equations of (collinear) motion [98]. The mass combination **H + HL** accentuates surface I behaviour while diminishing the surface II effect, whereas **L + HH** has the converse effect. The qualitative behaviour noted above remains unaltered.

A further significant refinement in understanding the controlling features of

the pes takes note of the fact that in the case of a late barrier-crest some part of the energy-barrier is located along the coordinate of approach. This further element was included in the picture by distinguishing between type "IIS" and "IIG" barriers, where S and G differentiate late-barriers approached by a Sudden or Gradual potential rise [97]. The gradual rise implies the existence of a significant fraction of the type II barrier in the coordinate of approach, with a corresponding requirement for a minimum reagent translational energy along with the (dominant) vibrational contribution.

A further dividend that accrues from the inclusion of this refinement is that it has the effect of tying in the considerations raised in this section regarding the favoured type of reagent energy for endothermic barrier crossing, with those described in section 2.2 in regard to the channelling of exothermic energy into product degrees of freedom. The portion of the (late) barrier to endothermic reaction that extends into the coordinate of approach for 'reverse' reaction, is the portion of the exothermic energy release that occurs in the coordinate of separation for 'forward' reaction; we are viewing the same hill from below and above. Similarly the reagent translational energy required for endothermic reaction is related to the translational energy derived from repulsive energy-release in the corresponding exothermic reaction. Since the pes is a single whole, it is to be hoped that the various indices of reactive behaviour bear an evident relationship to one another.

The "indices of reactive behaviour" referred to in the previous paragraph (see 2.2, 3.2 and 4.2) make frequent use of the collinear "diagnostic" pes. Since this allows for neither reagent nor product angular momenta, it gives no insight into the sources of product rotation (section 2.2), nor into the channelling of reagent rotation into motion across the barrier.

The experimentally observed dependence of reaction probability on J can plausibly be explained as follows [91]. In the great majority of reactions there will be a preferred orientation for the required close-approach of the attacking atom to the molecule under attack. With increased J, the time that the system spends in this orientation will decrease, as will the detailed rate constant, k(J). With further increase in J, the preferred orientation will be recovered at short intervals during the approach of A to BC, resulting in a reversal of the downward trend in k(J). At high J, the attacking atom responds to an average interaction around BC; k(J) would be expected to level off. There is, however, a further contributing factor at J sufficiently high that the rotational energy is significant in terms of the energy required for barrier-crossing; this is the effect of rotation in carrying the system across the barrier to reaction. If the barrier is "late", this would be expected to occur largely through vibration-rotation interaction; if "early" through the component of force along r_{AB} as BC rotates into A (see [72b] for the geometry of this collision).

These scenarios are speculative. What can be said with assurance is that the ratio of time spent along the approach coordinate to the rotational period of the molecule under attack will play an important role in the outcome of a potentially-reactive encounter, in addition to the energy vested in rotation.

5. FUTURE DIRECTIONS

This talk has described the development of one type of "state specified" chemistry, from which some simple lessons regarding reaction dynamics can be drawn. What we see obscurely today, we shall in the future see much more clearly through the more rigorous application of state-selection, an increase in the range of attributes being selected, and also an extension in the range of reactions amenable to study. All of this will add up to a maturation of the field of state-to-state chemistry.

In closing I mention two further approaches which could assist materially in the quest for understanding of the choreography of chemical reaction. In the first, attempts are being made to observe the molecular partners while they are, so to speak, on the stage, rather than immediately prior to and following the reactive dance. This we term "transition state spectroscopy" (TSS); it is a young but burgeoning field. In the second novel approach, the intention, stated a little grandiosely, is to have a hand in writing the script according to which the dynamics occurs; the reagents are aligned by the forces at a crystal surface and held in a fixed arrangement immediately prior to the initiation of the reaction by light, thus restricting the subsequent pattern of motion. This field of "surface aligned photochemistry" (SAP) has only very recently made its appearance. SAP may initiate reaction part way across the pes and hence is related to TSS, since the adsorbed reactants can be held together in configurations that locate them at the outset part way up the reactive barrier. In the SAP experiments performed till now the forces holding the reactants to the surface have been physisorptive.

These two approaches, TSS and SAP, will be briefly reviewed.

The impetus for transition state spectroscopy, TSS, came from a series of theoretical studies of the effect of laser fields on reactive encounters [102]. A variety of intriguing alterations in dynamics were predicted, exemplifying in the reactive domain the effects being explored at that date for non-reactive encounters under the heading of "laser assisted collisions". However, the laser powers thought to be required lay in the gigawatt to terawatt range (powers associated with the electrical breakdown of gases) so that the outlook for success appeared bleak.

It was pointed out that a simple alternative would be to look for emission from electronically-excited transition-state configurations ($ABC^{\ddagger *}$) [103]. (In reaction rate theory "transition states" are sets of intermediate configurations variously defined; in the spectroscopic context we use the term to denote the full range of configurations intermediate between reactants A + BC and products AB + C). An example is shown in fig. 33. In collisional line-broadening of Na* + NaX the wings of the atomic line emission would be due to the approach of Na* to NaX (moving from right to left in the figure) followed by emission of frequency ν_{em}. In TSS comparable wings should be observed due to the fact that every Na* is formed by separation from NaX (moving from left to right in the figure); separation can be preceded by emission at frequency ν_{em}. A simple calculation showed that the emission intensity at a ν_{em}, of ~1 cm-' bandwidth, would total $\sim 10^{-6}$x the chemiluminescent intensity of Na*, and that this

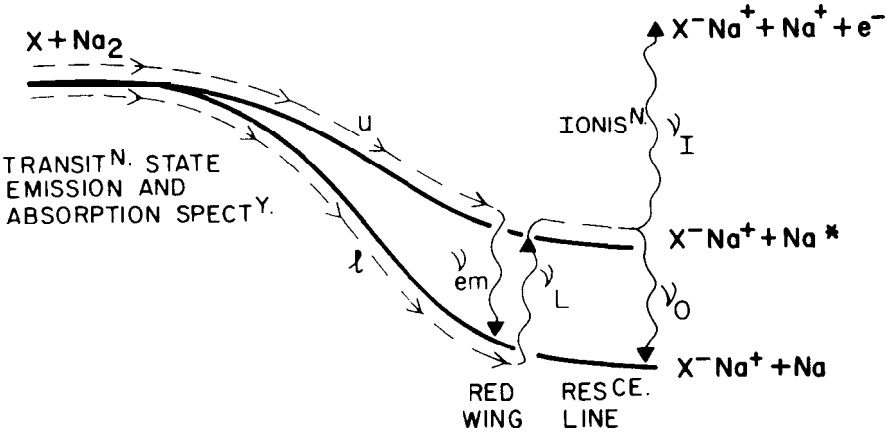

Figure 33. Illustration of transition state emission and absorption spectroscopy, in analogy to collisional line-broadening. The reaction is X + Na_2 → NaX + Na(*) (X = halogen). Reaction on the upper surface, u, leads to emission as the products separate (ν_{em} constitutes a red-shifted "wing" on the D-line at $\nu_{,}$). Reaction on the lower surface, 1, may be detected by laser absorption as products separate ($\nu_L < \nu_o$ in the illustration); absorption at ν_L may be evidenced by subsequent emission of Na* at $\nu_{,,}$ or by laser ionization of Na* using a second laser tuned to ν_I. From J.C. Polanyi, Faraday Disc. Chem. Soc., 67, 129 (1979).

should be measurable. Observation of wings of this intensity, having the appropriate kinetics, followed shortly thereafter [104]. Preliminary reports of similar measurements in absorption [105-107] have led to more definitive successes [108] at increasing levels of spectroscopic detail [109].

The relative intensity of the TSS at various ν_{em} or ν_L (corrected for changing transition moment, where warranted) will yield information concerning the relative times that the absorber, ABC‡, spends at successive configurations en *route* from reagents to products [110-112]. This is precisely the information that reaction dynamicists have sought to infer from a knowledge of reagent and product motions. The more direct approach of TSS suffers from the drawback that it is a spectroscopy of two pes rather than one, namely the reactive pes and the optically-linked pes (preferably a bound state) to which emission or absorption *occurs*. This complication need no *more* be fatal to TSS than it was to the study of stable molecules by electronic emission or absorption spectroscopy in decades past. It does however mean that as soon as our experimental virtuosity permits, we should turn our attention to the TSS of the simplest reactive systems, such as that involving only hydrogen atoms (H + H_2 → H $_3$‡ → H_2 + H) [111,112].

In regard to SAP (Surface Aligned Photochemistry), we can be brief. In the experiments performed to date [113], a submonolayer of H_2S was adsorbed in ultrahigh vacuum (UHV) on a single crystal of LiF(001), and was irradiated with ultraviolet (UV) at 193 and 222 nm coming from an excimer laser (5mJ/pulse). At low coverage (-0.01 monolayers) fastmoving H photofragments

were observed to leave the surface. From their energy and angular distribution these were clearly due to the uv photolysis of H_2S still held at the surface at the instant of photofragmentation. With increasing coverage (≥ 0.1 monolayers) the photoproducts included fast-moving H_2 formed in the reaction $H + H_2S \rightarrow H_2 + HS$. The yield of H_2 increased with coverage at a rate and to an extent that could only be explained by the reaction of photorecoiling H with *adsorbed* H_2S; accordingly the reaction is ascribed to SAP. The H_2 product is fast and directional.

This is a small first step along the way to inducing reactions under conditions where the range of reagent angles-of-approach and impact parameters is restricted by surface alignment and (by choice of crystal, crystal face and coverage) is controllable. A trajectory study [113] illustrates the simplified link between product attributes and reactive geometries that applies under these more disciplined conditions.

Even in the world of molecules the civilising influence of modest restraints is a cause for rejoicing.

ACKNOWLEDGMENTS

The research described here in so far as it relates to the work of my laboratory was performed over a thirty year period at the University of Toronto. It is a pleasure to express my indebtedness to my colleagues at this University - most especially to the late Prof. D.J. LeRoy who fostered this work from its inception - and to my students and postdoctoral associates whose talents, generosity and friendship have made this undertaking possible under fulfilling.

REFERENCES

1. M. Beutler and M. Polanyi, Z. Phys. Chem B1, 3 (1928); St. v. Bogdandy and M. Polanyi ibid. *1,* 21 (1928); M. Polanyi and G. Schay, ibid. *1, 30* (1928).
2. D.R. Bates and M. Nicolet, J. Geophys. Res. 55, 301 (1950).
3. G. Herzberg, J. Roy. Astron. Soc. Canada 4.5, 100 (1951).
4. J.D. McKinley, D. Garvin and M. Boudart, J. Chem. Phys. 23, 784 (1955); T.M. Cawthorn and J.D. McKinley, ibid. 2.5, 583 (1956).
5. F.J. Lipscomb, R.G.W. Norrish and B.A. Thrush, Proc. Roy. Soc. A 233, 455 (1956).
6. J.K. Cashion and J.C. Polanyi, J. Chem. Phys. 29, 455 (1958).
7. J.K. Cashion and J.C. Polanyi, J. Chem. Phys., 30, 1097 (1959); same authors Proc. Roy. Soc. (London) *A258, 529, 564,570* (1960).
8. A.L. Schawlow and C.H. Townes, Phys. Rev. *112* 1940 (1958); A.M. Prokhorov, Zh. Eksptl. i. Teor. Fiz. 34 1658 (1958) and Sov. Phys.-JETP 7, 1140 (1958).
9. J.C. Polanyi, Proc. Roy. Soc. (Canada) 54(C), 25 (1960); J. Chem. Phys. 34, 347 (1.961).
10. J.C. Polanyi, Applied Optics Supplement 2, 109 (1965).
11. C.K.N. Patel, W.L Faust, and R.A. McFarlane, Bull. Am. Phys. Soc. *119, 500* (1964); C.K.N. Pate1 and R.J. Kerl, Appl. Phys. Letts. *5,* 81 (1964); C.K. N. Patel, Phys. Rev. Letts. *12. 588* (1964).
12. J.V.V. Kasper and G.C. Pimentel, Phys. Rev. Lett., *14,352* (1965); G.C. Pimentel, Sci. Am., 214, 32 (1966).
13. P.E. Charters and J.C. Poianyi, Disc. Faraday. Soc 33. 107 (1962).
14. H.O. Pritchard, Trans. Faraday Soc., 33, 278 (1962).
15. J.C. Polanyi, Trans. Faraday Soc., 33, 279 (1962).
16. K.G. Anlauf, P.J. Kuntz, D.H. Maylotte, P.D. Pacey and J.C. Polanyi, Disc. Faraday Soc. 44, 183 (1967).
17. P.D. Pacey and J.C. Polanyi, J. Applied Optics, *JO,* 1725 (1971).
18. D.H. Maylotte, J.C. Polanyi and K.B. Woodall, J. Chem. Phys. 57, 1547 (1972).
19. K.G. Anlauf, D.S. Horne, R.G. Macdonald, J.C. Polanyi and K.B. Woodall, J. Chem. Phys. 57 1561 (1972).
20. J.D. Polanyi and K.B. Woodall, J, Chem. Phys. 57, 1574 (1972).
21. J.C. Polanyi and J.J. Sloan, J. Chem. Phys. 57, 4988 (1972).
22. F. London, *Problem der Modernen Physik* (Sommerfeld Festschrift) p. 104 (1928); Z. Elektrochem. 35, 552 (1924).
23. H. Eyring and M. Polanyi, Z. Physik. Chem. *B12, 279* (1931).
24. J.O. Hirschfelder and E. Wigner, J. Chem. Phys. 7, 616 (1929).
25. F.T. Wall, L.A. Hiller, and J. Mazur, J. Chem. Phys. 29,255 (1958).; ibid. 35, 1284 (1961).
26. N.C. Blais and D.L. Bunker, J. Chem. Phys., *37,* 2713 (1962); ibid. 39, 315 (1962).
27. J.C. Polanyi in *Transfert d'Energie dans les Gaz,* Ed. R. Stoops, p. 177-182, 526-528, Interscience Publishers, N.Y. (1962); J.C. Polanyi and S.D. Rosner, J. Chem. Phys. 38, 1028 (1963).
28. M.G. Evans and M. Polanyi, Trans. Faraday Soc., 35, 178 (1939).
29. For a review see B.S. Agrawala and D.W. Setser in *'Gas Phase Chemiluminescence and Chemi-ionization',* Ed. A. Fontijn, p. 157, Elsevier (1985).
30. B.M. Berquist, J.W. Bozzelli, L.S. Dzelzkalns, L.G. Piper and F. Kaufman, J. Chem. Phys. 76, 2976 (1982); B.M. Berquist, L.S. Dzelzkalns, F. Kaufman, ibid. 76, 2984 (1982); L.S. Dzelzkalns, and F. Kaufman, ibid. 77, 3508 (1982); L.S. Dzelzkalns and F. Kaufman, ibid. 79, 3836 (1983).
31. J.C. Weisshaar, T.S. Zwier and S.R. Leone, J. Chem. Phys. *75,* 4873 (1981); for a review see C.E. Hamilton and S.R. Leone in *'Gas Phase Chemiluminescence and Chemi-ionization' ,* Ed. A. Fontijn, p. 139, Elsevier (1985).

32. H.L. Welsh, C. Cumming, and E.J. Stansbury. J. Opt. Soc. Am. 41, 712 (1951); H.L. Welsh, E.J. Stansbury, J. Romanko, and T. Feldman, J. Opt. Soc. Am. 45, 338 (1955).
33. P.E. Charters, R.G. Macdonald, and J.C. Polanyi, Appl. Optics, IO, 1747 (1971).
34. N. Jonathan, C.M. Melliar-Smith, and D.H. Slater, Mol. Phys. 20, 93 (1971); N. Jonathan, C.M. Melliar-Smith, S. Okuda, D.M. Slater, and D. Timlin, Mol. Phys. 22, 561 (1971).
35. H.W. Chang and D.W. Setser, J. Chem. Phys. 58, 2298 (1973); D.J. Bogan and D.W. Setser, ibid. 64, 586 (1976).
36. J.C. Moehlmann and J.D. McDonald, J. Chem. Phys. 62, 3061 (1975); J.W. Hudgens and J.D. McDonald, ibid. 67, 3401 (1977).
37. P.M. Aker, D.J. Donaldson, and J.J. Sloan, J. Phys. Chem., 40, 3110 (1986).
38. D. Brandt, L.W. Dickson, L.N.Y. Kwan, and J.C. Polanyi, Chem. Phys. 39, 189 (1979); L.W. Dickson, Ph.D Thesis, Univ. of Toronto, 1982.
39. J.C. Polanyi and K.B. Woodall, J. Chem. Phys. 56, 1563 (1872).
40. J.H. Parker and G.C. Pimentel, J. Chem. Phys. *51,* 91 (1969); R.D. Coombe and G.C. Pimentel, ibid. 59, 251, 1535 (1973); M.J. Berry, ibid. 59, 6229 (1973).
41. K.G. Anlauf, J.C. Polanyi, W.H. Wong, and K.B. Woodall, J. Chem. Phys., 49, 5189 (1968).
42. D.M. Neumark, A.M. Wodtke, G.N. Robinson, C.C. Hayden, and Y.T. Lee, J. Chem. Phys. 82, 3045 (1985); D.M. Neumark, A.M. Wodtke, G.N. Robinson, C.C. Hayden, K. Shobotake, R.K. Sparks, T.P. Schaefer, and Y.T. Lee, J. Chem. Phys. 82, 3967 (1985).
43. R.B. Bernstein and R.D. Levine, J. Chem. Phys. 57, 434 (1972); R.B. Bernstein and R.D. Levine 'Advances in Atomic and Molecular Physics', Vol. 11 (Academic Press, New York, 1975); R.B. Bernstein and R.D. Levine in 'Modern Theoretical Chemistry', Vol. 3, Dynamics of Molecular Collisions, Part B, Ed. W.H. Miller (Plenum Press, New York, 1976) Chapter 7.
44. R.N. Zare and P.J. Dagdigian, Science, 185, 739 (1974).
45. "Multiphoton Spectroscopy of Molecules", by S.H. Lin, Y. Fujimura, H.J. Neusser, and E.W. Schlag (Academic Press, 1984).
46. P.M. Aker and J.J. Sloan, J. Chem. Phys. 85, 1412 (1986); P.M. Aker, J.J. Sloan, and J.S. Wright, Chem. Phys., In press (1986).
47. D.S. Perry and J.C. Polanyi, Chem. Phys. 12, 419 (1976).
48. K.G. Anlauf, P.E. Charters, D.S. Horne, R.G. Macdonald, D.H. Maylotte, J.C. Polanyi, W.J. Skrlac, D.C. Tardy, and K.B. Woodall, J. Chem. Phys. 53, 4091 (1970); H. Heydtmann and J.C. Polanyi, J. Appl. Optics, *10, 2738 (1971);* M.A. Nazar, J.C. Polanyi, and WJ. Skrlac, Chem. Phys. Letts. 29, 473 (1974); J.C. Polanyi and W.J. Skrlac, Chem. Phys. 23, 167 (1977); D. Brandt and J.C. Polanyi, Chem. Phys. 35, 23 (1978); ibid. 45, 65 (1980).
49. L.T. Cowley, D.S. Horne, and J.C. Polanyi, Chem. Phys. Letts., 12, 144 (1971).
50. A.M.G. Ding. L.J. Kirsch, D.S. Perry, J.C. Polanyi, and J.L. Schreiber, Faraday Disc. Chem. Soc., 55, 252 (1973).
51. J.C. Polanyi, J.L. Schreiber, and W.J. Skrlac, Faraday Disc. Chem. Soc. 67, 66 (1979).
52. J.C. Polanyi, J. Quant. Spectrosc. Radiat. Transfer 3, 471 (1963).
53. P.J. Kuntz, E.M. Nemeth, J.C. Polanyi, S.D. Rosner, and C.E. Young, J. Chem. Phys. 44, 1168 (1966).
54. D.S. Perry, J.C. Polanyi, and C. Woodrow Wilson Jr., Chem. Phys. 3. 317 (1974).
55. M.H. Mok and J.C. Polanyi, J. Chem. Phys. 52, 1451 (1969).
56. T.H. Dunning Jr, J. Phys. Chem. 88. 2469 (1984).
57. J.C. Polanyi, Disc Faraday Soc. 44, 293 (1967).
58. For a review see: J.C. Polanyi, Accounts, Chem. Res. 5, 161 (1972).
59. For a review see: J.C. Polanyi and J.L. Schreiber, Physical Chemistry - An Advanced Treatise, Vol. VIA. *Kinetics of Gas Reactions,* Eds., H. Eyring, W. Jost and D. Henderson (Academic Press, New York, 1974) Chap. 6, p. 383.

60. P.J. Kuntz, E.M. Nemeth, and J.C. Polanyi, J. Chem. Phys. *50,* 4607 (1969).
61. C.A. Parr, J.C. Polanyi, and W.H. Wong, J. Chem. Phys. 585 (1973).
62. J.T. Muckerman, J. Chem. Phys. 54, 1155 (1971); ibid. 56, 2997 (1972); ibid. 57, *3388* (1972).
63. J.C. Polanyi and J.L. Schreiber, Chem. Phys. Letts. 29, 319 (1974).
64. J.C. Polanyi and J.L. Schreiber, Faraday Disc. Chem. Soc. 62, 267 (1977).
65. C.F. Bender, S.V. O'Neill, P.K. Pearson, and H.F. Schaefer III, Science 176, 1412 (1972).
66. H.F. Schaefer III, J. Phys. Chem. 89, 5336 (1985).
67. D.S. Perry and J.C. Polanyi, Chem. Phys. 12, 419 (1976).
68. P.J. Kuntz, M.H. Mok, and J.C. Polanyi, J. Chem. Phys. 50,4623 (1969).
69. D.R. Herschbach, Faraday Disc. Chem. Soc., 55,233 (1973).
70. M.G. Prisant, C.T. Rettner, and R.N. Zare, J. Chem. Phys. *81, 2699 (1984).*
71. M.D. Pattengill and J.C. Polanyi, Chem. Phys. 3, 1 (1974).
72. (a) N.H. Hijazi and J.C. Polanyi, J. Chem. Phys. 63, 2249 (1975); (b) N.H. Hijazi and J.C. Polanyi, Chem. Phys. *11,* 1 (1975).
73. J.J. Valentini, M.J. Coggiola, and Y.T. Lee, J. Am. Chem. Soc. 98, 853 (1976); Faraday Disc., Chem. Soc., 62, 232 (1977).
74. J.W. Hudgens and J.D. McDonald, J. Chem. Phys. 67, 3401 (1977).
75. L.T. Cowley, D.S. Horne, and J.C. Polanyi, Chem. Phys. Letts. *12,* 144 (1971).
76. B.A. Blackwell, J.C. Polanyi, and J.J. Sloan, Chem. Phys. 24, 25 (1977).
77. D.J. Douglas and J.C. Polanyi, Chem. Phys. *16,* 1 (1976).
78. R.D. Coombe and G.C. Pimentel, J. Chem. Phys. 59, 1535 (1973).
79. D.L. Thompson, J. Chem. Phys. 56, 3570 (1972).
80. J.C. Polanyi, Faraday Disc. Chem. Soc. 55, 389 (1973).
81. J.C. Polanyi, J.L. Schreiber, and J.J. Sloan, Chem. Phys. 9, 403 (1975).
82. J.C. Polanyi, J.J. Sloan, and J. Wanner, Chem. Phys. 13, 1 (1976).
83. K.G. Anlauf, D.H. Maylotte, J.C. Polanyi, and R.B. Bernstein, J. Chem. Phys. *51,* 5716 (1969).
84. J.C. Polanyi, and D.C. Tardy, J. Chem. Phys. *51,* 5717 (1969).
85. D.S. Perry, J.C. Polanyi and C. Woodrow Wilson Jr., Chem. Phys. Letts. 24, 484 (1974).
86. T.J. Odiorne, P.R. Brooks, and J.V.V. Kasper, J. Chem. Phys. 55, 1980 (1971; J.G. Pruett, F.R. Grabiner, and P.R. Brooks, ibid. 63, 3335 (1974); J.G. Pruett, F.R. Grabiner, and P.R. Brooks, ibid. 63, 1173 (1975).
87. A Gupta, D.S. Perry, and R.N. Zare, J. Chem. Phys. 72, 6237, 6250 (1980).
88. F. Heismann and H.J. Loesch, Chem. Phys. *64,* 43 (1982).
89. D.J. Douglas, J.C. Polanyi, and J.J. Sloan, J. Chem. Phys. 59, 6679 (1973).
90. F.E. Bartozek, B.A. Blackwell, J.C. Polanyi, and J.J. Sloan, J. Chem. Phys 74 3400 (1981).
91. B.A. Blackwell, J.C. Polanyi, and J.J. Sloan, Chem. Phys. 30,299 (1978).
92. H.H. Dispert, M.W. Geis, and P.R. Brooks, J. Chem. Phys. 70, 5317 (1979).
93. M.Hoffmeister, L. Potthast, and H.J. Loesch, Book of Abstracts, XII International Conf. on the Physics of Elektronic and Atomic Collisions, Gatlinburg (1981).
94. J.C. Polanyi and W.H. Wong, J. Chem. Phys. *51,* 1439 (1969).
95. J.W. Duff and D.G. Truhlar, J. Chem. Phys. *62,* 2477 (1975).
96. G.L. Hofacker and R.D. Levine, Chem. Phys. Letts. *9,* 617 (1971).
97. J.C. Polanyi and N. Sathyamurthy, Chem. Phys. *33,* 287 (1978).
98. B.A. Hodgson and J.C. Polanyi, J. Chem. Phys. *55,* 4745 (1971).
99. M.H. Mok and J.C. Polanyi, J. Chem. Phys. *53,* 4588 (1970).
100. G.S. Hammond, J. Amer. Chem. Soc. 77, 334 (1955).
101. J. C. Polanyi, J. Phys. Chem. 31, 1338 (1959).
102. (a) T.F. George, J. Phys. Chem. *86,* 10 (1982) and references therein; (b) A.M.F. Lau, Phys. Rev. *A13,* 139 (1976); 14, 279 (1976); Phys. Rev. Lett. 43, 1009 (1978);

Phys. Rev A22, 614 (1980); (c) V.S. Dubov, L.I. Gudzenko, L.V. Gurvich and S.I. Yakovlenko, Chem. Phys. Lett. 45, 330 (1977); S.I. Yakovlenko, Sov. J. Quantum Electron, 8, 151 (1977); (d) A.E. Ore1 and W.H. Miller, Chem. Phys. Lett. 57, 362 (1979); J. Chem. Phys. 70, 4393 (1979); (e) J.C. Light and A. Altenberger-Siczek, ibid. 70, 4108 (1979).

103. J.C. Polanyi, Faraday Disc. Chem. Soc. 67, 129 (1979).
104. P. Arrowsmith, F.E. Bartoszek, S.H.P. Bly, T. Carrington, Jr., P.E. Charters, and J.C. Polanyi, J. Chem. Phys. 73, 5895 (1980); H.-J.. Foth, J.C. Polanyi, and H.H. Telle, J. Phys. Chem. 86, 5027 (1982); P. Arrowsmith, S.H.P. Bly, P.E. Charters, and J.C. Polanyi, J. Chem. Phys. 79, 283 (1983).
105. P. Hering, P.R. Brooks, R.F. Curl Jr., R.S. Judson, and R.S. Lowe, Phys. Rev. Lett. 44, 657 (1980); P.R. Brooks, R.F. Curl, and T.C. Maguire, Ber. Bunsenges. Phys. Chem. 86, 401 (1982).
106. H.P. Grieneisen, H. Xue-Jing, and K.L. Kompa, Chem. Phys. Letts. 82, 421 (1981).
107. J.K. Ku, G. Inoue, and D.W. Setser, J. Phys. Chem. 87, 2989 (1983).
108. T.C. Maguire, P.R. Brooks R.F. Curl, J.H. Spence, and S. Ulrick, J. Chem. Phys. 85, 844 (1986); T.C. Maguire, P.R. Brooks, R.F. Curl, J.H. Spence, and S. Ulrick, Phys. Rev. A34, 4418 (1986).
109. P.D. Kleiber, A.M. Lyyra, K.M. Sando, S.P. Heneghan, and W.C. Stwalley, Phys. Rev. Letts. 54, 2003 (1985); P.D. Kleiber, A.M. Lyyra, K.M. Sando, V. Zafiropolos, and W.C. Stwalley, J. Chem. Phys. 85, 5493 (1986).
110. J.C. Polanyi and R.J. Wolf, J. Chem. Phys. 75, 5951 (1981).
111. H.R. Mayne, R.A. Poirier, and J.C. Polanyi, J. Chem. Phys. *80,* 4025 (1984); H.R. Mayne, J.C. Polanyi, N. Sathyamurthy, and S. Raynor, ibid. 88, 4064 (1984).
112. V. Engel, Z. Bacic, R. Schinke, and M. Shapiro, J. Chem. Phys. 82, 4844 (1985); V. Engel and R. Schinke, Chem. Phys. Letts. 122, 103 (1985).
113. E.B.D. Bourdon, J.P. Cowin, I. Harrison, J.C. Polanyi, J. Segner, C.D. Stanners, and P.A. Young, J. Phys. Chem. 88, 6100 (1984); E.B.D. Bourdon, P. Das, I. Harrison, J.C. Polanyi, J. Segner, C.D. Stanners, R.J. Williams, and P.A. Young, Faraday Disc. Chem. Soc. 82, 343 (1986).